Late Miocene high and rapid surface uplift and its erosional response in the Andes of central Chile (33°–35°S)

Marcelo Farías,[1,2,3] Reynaldo Charrier,[1] Sébastien Carretier,[2] Joseph Martinod,[2] Andrés Fock,[1,4] David Campbell,[1] Joaquín Cáceres,[1] and Diana Comte[3]

Received 6 September 2006; revised 29 August 2007; accepted 4 October 2007; published 17 January 2008.

[1] We address the question of the late Cenozoic geomorphological evolution of the central Chile Andes (33°–35°S), using uplift markers, river incision, previous and new ages of volcanic bodies, and new fission track ages. The uplift markers consist of relicts of high elevated peneplains that evidence >2 km of regional surface uplift lasting ~2 Ma with variable amount along an E-W transect. The eastern Coastal Cordillera was uplifted 1.5–2.1 km at 33–34°S and <1 km at 35°S, the western Principal Cordillera was uplifted ~2 km, and the central eastern Principal Cordillera was uplifted >2.5 at 33°45′S and ~1.5 km at 34°30′S. Erosional response to uplift was characterized by the retreat of a sharp knickpoint with celerities between 10 and 40 mm a^{-1}. Extrapolation using a stream power law shows that uplift began shortly before 4 Ma or at 10.5–4.6 Ma (7.6 Ma central age) depending on the morphostructural units involved. The first alternative implies simultaneous uplift of the continental margin. The second model (the most reliable one) implies that the uplift affected together the eastern Coastal Cordillera and the Principal Cordillera, while the rest of the western fore arc subsided. This regional uplift can be mostly balanced by crustal thickening resulting from coeval shortening related to the out-of-sequence thrusting event in the Principal Cordillera and the uplift of the Frontal Cordillera. Simultaneously, emplacement of the southern edge of the flat slab subduction zone might have partially contributed to this uplift event.
Citation: Farías, M., R. Charrier, S. Carretier, J. Martinod, A. Fock, D. Campbell, J. Cáceres, and D. Comte (2008), Late Miocene high and rapid surface uplift and its erosional response in the Andes of central Chile (33°–35°S), *Tectonics*, *27*, TC1005, doi:10.1029/2006TC002046.

[1]Departamento de Geología, Universidad de Chile, Santiago, Chile.
[2]Laboratoire de Mécanismes et Transferts en Géologie, IRD, CNRS, Université de Toulouse, Toulouse, France.
[3]Departamento de Geofísica, Universidad de Chile, Santiago, Chile.
[4]Sociedad Quimica y Minera Salar S.A., Antofagasta, Chile.

0278-7407/08/2006TC002046

1. Introduction

[2] It is widely recognized that river incision into bedrock controls landscape evolution and denudation by setting the base level to the hillslopes and by linking climate and tectonics to the watershed evolution [e.g., *Burbank et al.*, 1996; *Pazzaglia et al.*, 1998; *Whipple and Tucker*, 1999]. Rivers respond to uplift by upstream propagation of a perturbation (process known as ''knickpoint retreat'') formed in the border of the uplifted surface, which is the zone where channel slope initially increases. Knickpoint retreat develops as two end-member models in detachment-limited systems (i.e., in drainage systems where fluvial erosion is limited by the detachment of bedrock material), namely, parallel retreat and slope replacement models (Figure 1) [e.g., *Gardner*, 1983; *Seidl and Dietrich*, 1992]. Therefore erosion is not necessary coeval to uplift, but actually it can be somewhat delayed depending on stream hydraulic behavior. Considering that mountain building is commonly inferred from erosional and sedimentary records, this delay may lead to misinterpretations of uplift timing. Moreover, climatic effects can produce changes on erosion rates [e.g., *Molnar*, 2004; *Babault et al.*, 2005], therefore it could induce changes on the timing of this delay.

[3] In the central Chile Andes (33°–35°S, Figures 2c and 3), modern orogeny began in the lower Miocene as a result of inversion of a late Eocene-Oligocene extensional basin (Abanico basin) [e.g., *Charrier et al.*, 1996, 2002; *Godoy and Lara*, 1994; *Godoy et al.*, 1999]. Mountain building was characterized by crustal thickening (evidenced by geochemical signatures of igneous deposits in the western and central sectors of the range [*Nyström et al.*, 1993]) and by shortening mostly accommodated in its eastern flank [e.g., *Giambiagi and Ramos*, 2002; *Fock et al.*, 2005]. Although some deformed rocks reach more than 5000 m above sea level (asl), the highest peaks mainly correspond to volcanoes. This mixed volcanic-tectonic landscape is presently dissected by valleys as deep as 3000 m.

[4] In spite of this impressive landscape, relief evolution of this region is almost unknown, in contrast with its petrologic and structural history. Previous works introduced the concept of a major exhumation event in the late Neogene [e.g., *Skewes and Holmgren*, 1993; *Skewes and Stern*, 1996; *Maksaev et al.*, 2003, 2004], emphasizing the importance of denudation during mineralization in the two world-class porphyry copper deposits of this zone (El Teniente and Río Blanco-Los Bronces, Figure 2).

[5] The objective of this paper is (1) to present evidence for rapid and high magnitude surface uplift in the central

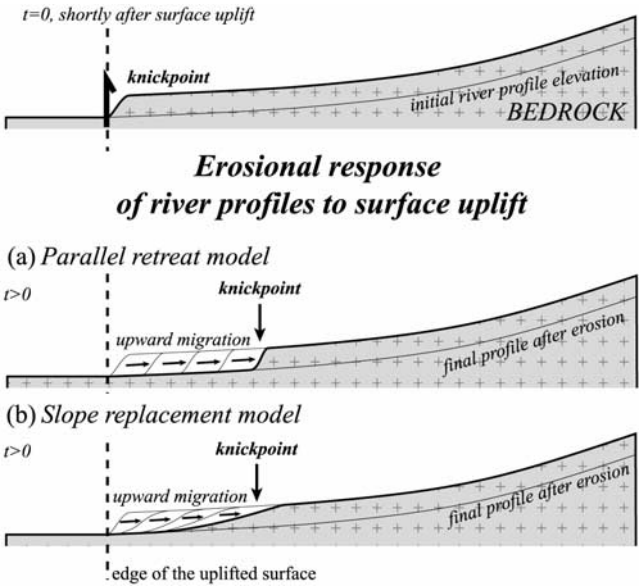

Figure 1. Knickpoint propagation along longitudinal river profiles. Surface uplift generates a knickpoint that propagates upstream. Knickpoint retreat is represented by two end-members models: (a) parallel retreat and (b) slope replacement. Modified after *Gardner* [1983] and *Seidl and Dietrich* [1992].

Chile Andean Cordillera during the late Neogene and (2) to examine how watersheds evolved and erosion propagated into the main range. Timing of erosional events is constrained by ages of igneous deposits and fission track thermochronology. Finally, we estimate the onset of surface uplift and discuss its implications for the evolution of Andean margin in central Chile.

2. Regional Settings

[6] The Andes are the result of tectonic shortening and magmatic activity due to an almost uninterrupted subduction since Jurassic times [e.g., *Coira et al.*, 1982; *Jordan et al.*, 1983; *Allmendinger*, 1986; *Isacks*, 1988]. Current plate convergence between the Nazca and South America plates is oriented N78°E and occurs at a rate of ~8 cm a^{-1} (Figure 2) [*Gripp and Gordon*, 2002].

[7] South of 33°S, the continental border changes its orientation from N-S, to the north, to NNE-SSW, to the south (Maipo orocline, Figure 2). In this region, the Andes are segmented into five trench-parallel continental morphostructural units (Figures 2 and 3), from west to east: Coastal Cordillera, Central Depression, Principal Cordillera (where the volcanic arc is emplaced), Frontal Cordillera, and Foreland. For the discussion related to the uplift patterns, we subdivided the Principal Cordillera into western, central, and eastern Principal Cordillera according to the geological features that we describe in the next paragraphs (Figure 2). We also subdivided the Coastal Cordillera into an eastern (eastern Coastal Cordillera) and a western domain (western Coastal Cordillera).

[8] The western Coastal Cordillera corresponds to a Paleozoic-Jurassic metamorphic and intrusive basement covered by late Miocene to Recent marine deposits (Figure 2b). Marine terraces of probable Pleistocene age were constructed on this part of the Coastal Cordillera [see *Wall et al.*, 1996, and references therein]. In turn, the eastern Coastal Cordillera is made up by east dipping late Jurassic to late Cretaceous stratified sequences and Cretaceous granites [*Thomas*, 1958].

[9] The Central Depression consists of a Quaternary sedimentary and ignimbritic cover. This cover has a maximum thickness of ~500 m beneath the Santiago valley [*Araneda et al.*, 2000]. The basement of the Central Depression corresponds to Mesozoic rocks in its western side and Cenozoic rocks in its eastern side (Figure 2). According to gravimetrical analysis in the Santiago depression [*Araneda et al.*, 2000], this basement presents a river network morphology, where some summits reach the surface forming isolated hills. Those hills commonly consist of intrusive rocks. Basement rocks also crop out in junction ridges (hereafter referred to as "junctions") between the Coastal Cordillera and Principal Cordillera (Figure 3).

[10] The western Principal Cordillera consists of Cenozoic sequences that only exhibit important deformation in its westernmost flank (Figure 2c). The central Principal Cordillera also consists of Cenozoic rocks, but here the deformation is more intense. The eastern Principal Cordillera is almost exclusively composed of Mesozoic deformed sequences. Both the central Principal Cordillera and the eastern Principal Cordillera constitute the fold-and-thrust belt in this region.

[11] The Andean evolution in central Chile (33°–35°S) comprises multiple stages of extension and contraction [*Charrier et al.*, 1996, 2007]. The last extensional event occurred in the Eocene-Oligocene, forming a basin where the Abanico Formation was deposited (mainly volcanic and volcaniclastic) [*Charrier et al.*, 2002, 2005; *Godoy and Lara*, 1994; *Godoy et al.*, 1999]. The Abanico basin extended from approximately the central axis of the Central Depression up to the Chilean eastern Principal Cordillera. On both margins, the Abanico Formation is presently separated from the Mesozoic sequences by inverse faults that correspond to basin-bounding normal faults partially inverted (Figure 2c). *Charrier et al.* [2002] proposed that inversion occurred between 21 and 16 Ma, which mainly affected the basin borders. This process led to the formation of a new basin in the central part of the western Principal Cordillera that was filled by the Farellones Formation (that represents the Miocene volcanic arc [e.g., *Vergara et al.*, 1988; *Elgueta et al.*, 1999; *Godoy et al.*, 1999; *Charrier et al.*, 2002]). The Farellones Formation exhibits growth strata within its lower portion because of basin inversion; in contrast, layers younger than ~16 Ma remain almost undeformed [*Fock et al.*, 2005]. This can be explained by the eastward migration of deformation toward the eastern Principal Cordillera at that time. In this area the deformation continued until ~8.5 Ma, accommodating most of the

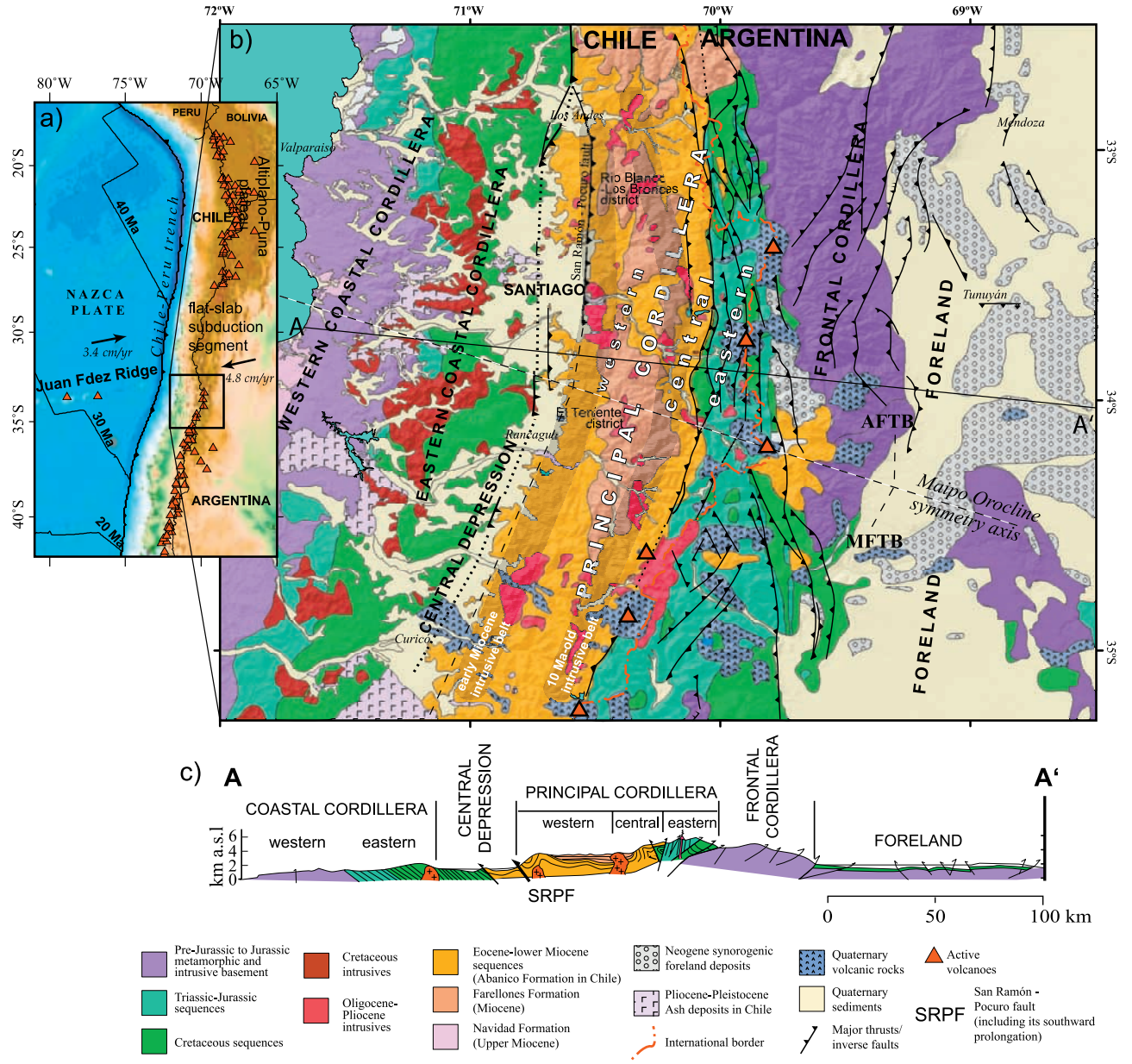

Figure 2. (a) Location of the study region. (b) Geological map of the Andes of central Chile and Argentina. Only main thrusts active during the Neogene are plotted. (c) Simplified geological profile at the latitude of Santiago. The Maipo orocline delimits the Aconcagua (AFTB) and the Malargüe (MFTB) fold-and-thrust belts. Absolute plate velocity in Figure 2a is after *Gripp and Gordon* [2002], whereas Figures 2b and 2c are based on the work by *Servicio Geológico Minero Argentino* [1997], *Servicio Nacional de Geología y Minería* [2002], *Giambiagi et al.* [2003], and *Fock et al.* [2005].

shortening along the N-S trending Aconcagua fold-and-thrust belt, north of 34°15′S, and along the NNE-SSW Malargüe fold-and-thrust belt, south of this latitude (Figure 2) [*Giambiagi and Ramos*, 2002; *Giambiagi et al.*, 2003; *Fock et al.*, 2005]. Between ~8.5 and ~4 Ma, high-angle reverse faults uplifted the Frontal Cordillera [*Giambiagi et al.*, 2003]. At this time, out-of-sequence thrusts emplaced in the central and eastern Principal Cordillera, accommodating ~25 km of shortening at 33.5°S [*Giambiagi and Ramos*, 2002]. After 4 Ma, deformation migrated farther east to the foreland. At the present, the eastern basin-bounding fault system of the Abanico basin is still active [*Farías et al.*, 2006a], but Harvard centroid moment tensor (CMT) focal mechanisms show almost exclusively strike-slip earthquakes. During these tectonic events, the Mesozoic series situated in the eastern Coastal Cordillera and western

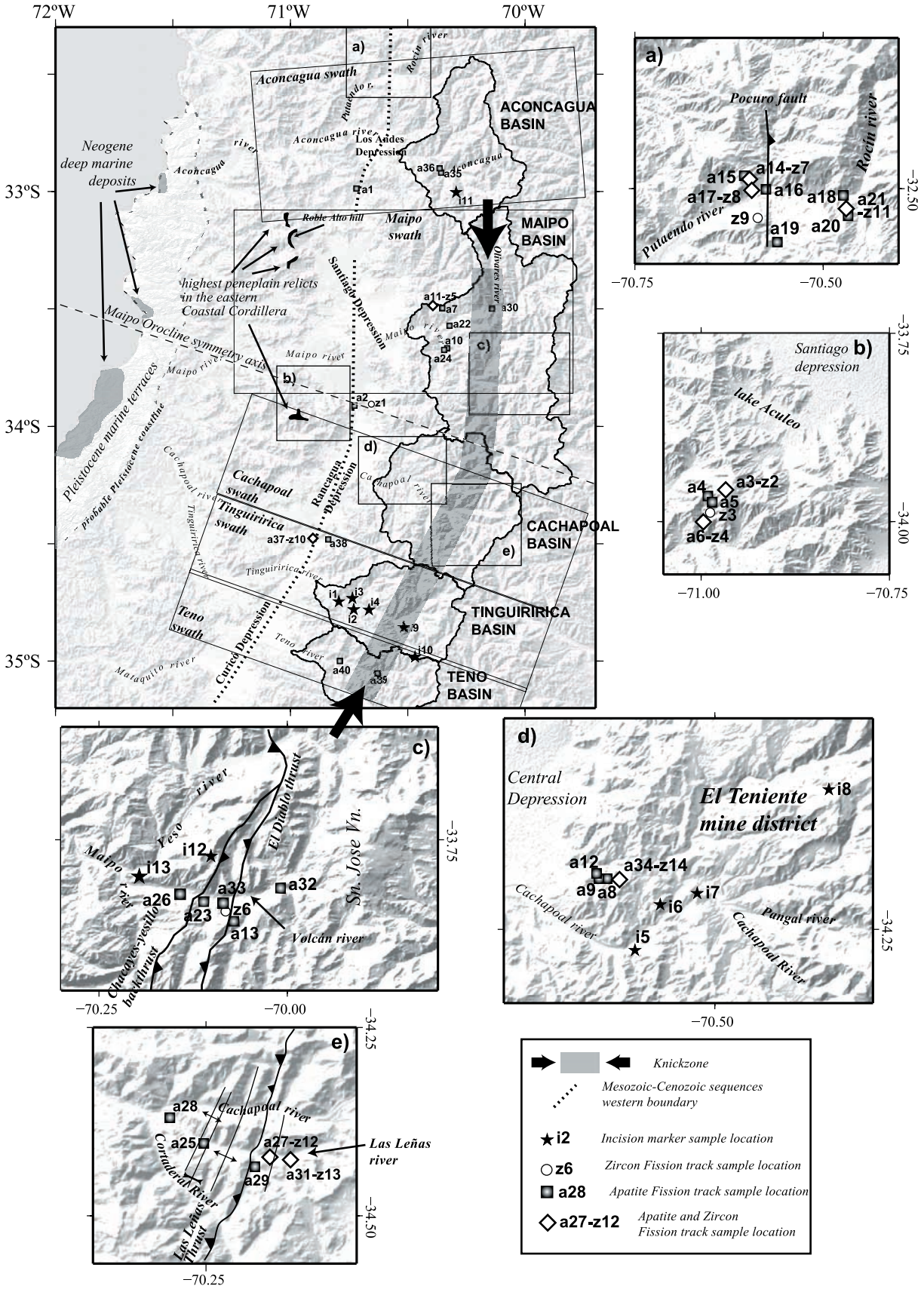
72ºW
71ºW
70ºW
33ºS
34ºS
35ºS
Aconcagua swath
Aconcagua river
Rocin river
Putaendo r.
Los Andes Depression
ACONCAGUA BASIN
Neogene deep marine deposits
Aconcagua river
Roble Alto hill
Maipo swath
MAIPO BASIN
highest peneplain relicts in the eastern Coastal Cordillera
Santiago Depression
Olivares river
Maipo Orocline symmetry axis
Maipo river
Pleistocene marine terraces
probable Pleistocene coastline
Cachapoal river
Cachapoal swath
Tinguiririca swath
Rancagua Depression
CACHAPOAL BASIN
Tinguiririca river
TINGUIRIRICA BASIN
Teno swath
Curicó Depression
Teno river
Mataquito river
TENO BASIN
a)
b)
c)
d)
e)
Pocuro fault
Putaendo river
Santiago depression
lake Aculeo
Central Depression
El Teniente mine district
Cachapoal River
Pangal river
Yeso river
El Diablo thrust
San José Vn.
Volcán river
Chacayes-Yesillo backthrust
Cortaderal River
Las Leñas river
Las Leñas Thrust
−33.75
−34.00
−32.50
−71.00
−70.75
−70.50
−70.25
−70.00
−34.25
−34.50
Knickzone
Mesozoic-Cenozoic sequences western boundary
i2 Incision marker sample location
z6 Zircon Fission track sample location
a28 Apatite Fission track sample location
a27-z12 Apatite and Zircon Fission track sample location

Figure 3

Central Depression were not subjected to major deformation, being only tilted eastward forming a gentle homocline (Figure 2c) [*Thomas*, 1958].

[12] During the Neogene, granitic intrusions were emplaced forming two orogen-parallel belts, namely, a lower Miocene belt in the westernmost Principal Cordillera, and a ~10 Ma old belt farther east (Figure 2). The latter separates the almost undeformed Miocene volcanites of the western Principal Cordillera from the deformed Cenozoic series in the central Principal Cordillera (Figures 2b and 3). In addition, magmatic activity migrated ~15 km to the west from the ~10 Ma old intrusive belt at 8–4 Ma, coeval with the emplacement of granitic bodies close to the present-day volcanic arc (i.e., 15–20 km to the east from the 10 Ma old belt) [see *Deckart et al.*, 2005; *Maksaev et al.*, 2004; *Kay et al.*, 2005, and references therein]. The western "arc" hosted high concentration of copper and molybdenum, forming the two giant porphyry copper deposits of central Chile (El Teniente and Río Blanco–Los Bronces, Figure 2). In addition to high ore concentration, geochemistry departs considerably from "normal arcs" compositions, showing adakitic-like signatures [*Rabbia et al.*, 2003; *Reich et al.*, 2003] and signals of asthenospheric source [*Kay et al.*, 1991, 2005; *Kay and Mpodozis*, 2001; *Stern and Skewes*, 1995, 2004; *Mathur et al.*, 2000]. In turn, the "eastern arc" presents "normal arc" geochemical signatures [*Stern and Skewes*, 1995; *Kurtz et al.*, 1997; S. M. Kay and A. Kurtz, Magmatic and tectonic characterization of the El Teniente region, Chilean Nacional Copper Corp., unpublished report, 1995], suggesting that porphyry copper-related magmatism did not correspond to the in the stricter sense arc and that two arcs coexisted. This process would have happened at the same time with the settlement of the southern edge of the flat slab subduction zone immediately north of 33°S [see *Yáñez et al.*, 2001, and references therein].

3. Main Morphological Features

[13] The Chilean Principal Cordillera extends up to the Pacific-Atlantic drainage divide. Maximum elevations are located there and consist in part of volcanic edifices as high as 6800 m asl. In the western Principal Cordillera, elevation diminishes to 2500–3000 m asl. Altitudes of the Principal Cordillera also diminish gradually to the south (Figure 4). This feature is also present in the Coastal Cordillera, where maximum elevations decrease from 2100 m at 33°S to 1000 m at 35°S.

[14] Five major drainage basins cross the entire Principal Cordillera in central Chile. From north to south, they receive the name of their main rivers: Aconcagua, Maipo, Cachapoal, Tinguiririca and Teno (Figure 3). Catchment areas differ (Table 1) and seem to be controlled by the presence of volcanic edifices. However, the Hack's law parameters (an empirical relationship between the stream length and the area of their basins [*Hack*, 1957]) for each basin are relatively similar (Table 1).

[15] Along each valley, main rivers are mostly alluvial channels where bedrock is not exposed. Only along the ~10 Ma old intrusive belt, rivers incise directly the bedrock. This feature spatially coincides with the junction of several tributaries (Figure 3) and with the increase in local channel slope (Figure 4).

[16] The valleys in the central Principal Cordillera and eastern Principal Cordillera are U-shaped, evidencing the influence of glaciations. Hillslope mass wasting locally dams the channels forming lakes. Mass wasting also remobilized moraine glacial deposits [e.g., *Abele*, 1984; C. Darwin, Letter 501 to J. D. Hooker in October 12th 1849, in *More Letters of Charles Darwin: A Record of His Work in a Series of Hitherto Unpublished Letters*, edited by F. Darwin and A. C. Seward, 1903, available at http://charles-darwin.classic-literature.co.uk/more-letters-of-charles-darwin-volume-ii/] being probably enhanced by shallow seismic activity in this part of the Principal Cordillera [*Farías et al.*, 2006a].

[17] The valleys in the western Principal Cordillera present alluvial rivers with alluvial terraces and volcanic deposits. This zone does not exhibit major evidence for glacial influence, except near the ~10 Ma old intrusive belt, where glacial deposits and landforms appear in some valley bottoms [*Borde*, 1966].

[18] Longitudinal river profiles systematically show bedrock knickpoints along the ~10 Ma old granodioritic belt (Figure 4). Although this belt is the western edge of the fold-and-thrust belt, knickpoints suggests a higher resistance to erosion of the granitic rocks than the encasing stratified rocks. In addition, glaciers advanced down to this zone. This feature was described by *Borde* [1966] in the Maipo basin, who interpreted it as a "verrou glacier" (zone where the presence of more resistant rocks produced a local increase on elevation and diminution of channel width along a glacial trough). At the exit into the Central Depression, rivers (that behave as alluvial channels) also exhibit knickpoints (Figure 4). This has been correlated with recent west vergent thrusting in the cordilleran front in Santiago along the San Ramón-Pocuro fault [*Rauld et al.*, 2006]. However, south of the Santiago depression (Figure 3), the mountain front is less sharp and knickpoints are better correlated with the lower Miocene intrusive belt. This feature suggests a mixed tectonic-lithologic control on evolution of the western edge of the Principal Cordillera.

[19] In the Central Depression and Coastal Cordillera, main rivers are characterized by a minor channel slope and by an alluvial bed. Bedrock rivers appear only and almost

Figure 3. Main morphological features of central Chile and sample locations. The main mountain drainage basins are indicated: Aconcagua, Maipo, Cachapoal, Tinguiririca, and Teno. Dotted line in the Central Valley corresponds to the western boundary of the Abanico basin (0 km reference). The ~10 Ma old intrusive belt is shown in order to display the separation between the central and western Principal Cordillera. Swath box shown are those displayed in the Figure 4. (a)–(e) Detailed regions showing the location of some samples used in this work.

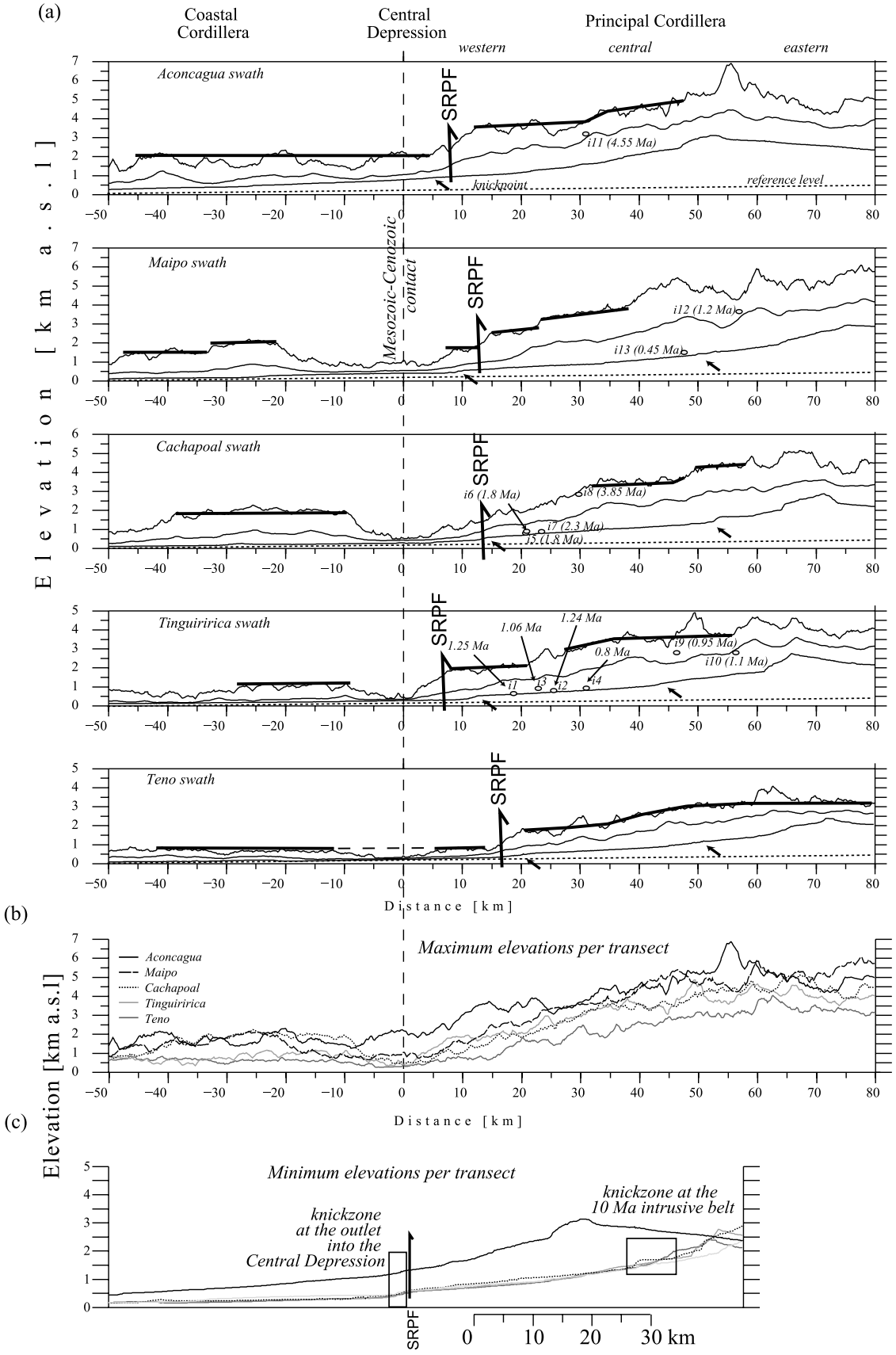
(a)
Coastal Cordillera
Central Depression
Principal Cordillera
western
central
eastern
Aconcagua swath
Maipo swath
Cachapoal swath
Tinguiririca swath
Teno swath
SRPF
Mesozoic-Cenozoic contact
i11 (4.55 Ma)
i12 (1.2 Ma)
i13 (0.45 Ma)
i6 (1.8 Ma)
i8 (3.85 Ma)
i7 (2.3 Ma)
i5 (1.8 Ma)
1.25 Ma
1.06 Ma
1.24 Ma
0.8 Ma
i9 (0.95 Ma)
i10 (1.1 Ma)
i1
i3
i2
i4
knickpoint
reference level
Elevation [km a.s.l]
Distance [km]
(b)
Maximum elevations per transect
Aconcagua
Maipo
Cachapoal
Tinguiririca
Teno
Elevation [km a.s.l]
Distance [km]
(c)
Minimum elevations per transect
knickzone at the outlet into the Central Depression
knickzone at the 10 Ma intrusive belt
SRPF
0 10 20 30 km

Figure 4

Table 1. Morphometry of Main Mountain Catchments in Central Chile

Mountain Drainage Basin	Drainage Area, m^2	Hack's Law Exponent h[a]	Hack's Law Constant k_a, m^{2-h}	R^2
Aconcagua	2.08×10^9	1.71	8.60	0.97
Maipo	4.95×10^9	1.88	2.43	0.96
Cachapoal	2.72×10^9	1.75	6.02	0.95
Tinguiririca	1.82×10^9	1.66	15.18	0.98
Teno	1.42×10^9	1.49	91.72	0.98
Mean values[b]		1.76	6.12	

[a]Hack's law relates the drainage area to the length of the main river along the watershed. See also section 5.2.
[b]Calculated from values of the Maipo, Cachapoal, and Tinguiririca basins.

systematically in a 20- to 40-km-wide belt adjacent to the coastline in the western Coastal Cordillera, evidencing recent surface uplift of this zone (Figure 3).

4. Evidence for Regional Surface Uplift

4.1. Emergence of Bathyal Deposits in the Western Coastal Cordillera

[20] Near the coast at 33°–34°S (Figures 2, 3, and 5), *Encinas et al.* [2006a, 2007] and *Finger et al.* [2007] described lower bathyal deposits overlain by shallow water sediments, which show at least 2 km of uplift occurring in Pliocene times. This process has been observed as far as 45°S [*Encinas et al.*, 2007; *Melnick and Echtler*, 2006].

[21] Emergence of bathyal deposits to shallow water environment would have concluded at the Zanclean [*Encinas et al.*, 2006a, 2006b, 2007]. The date of emersion is interpreted by (1) a laharic deposit overlying the bathyal deposits and (2) by foraminifers contained in the deep facies succession and shallow water deposits. *Encinas et al.* [2006b] reported three K-Ar ages for the laharic deposit (4.2 ± 0.8, 4.7 ± 0.4, and 7.7 ± 1.0 Ma) and one more reliable Ar/Ar age (2.7 ± 0.3 Ma total gas age). Likewise, foraminifers date the bathyal deposits (at 34°S) between 10.9 and 4.4 Ma [*Finger et al.*, 2007]. Therefore more than 2 km of uplift would have been occurred after 4.4 (youngest age for the bathyal deposits) and likely prior to 2.7 Ma (oldest age for the deposition of the lahar).

[22] These deposits and their bedrock constitute the floor of Pleistocene marine terrace surfaces [see *Wall et al.*, 1996, and references therein]. The present-day elevation of these surfaces represents a surface uplift of ~400 m after the great emergence described above. The uplift of these terraces has been controlled by vertical parallel-to-the-coastline faults [*Rodríguez et al.*, 2007], forming the 20–40 km wide belt where rivers cut directly on bedrock (Figure 3).

[23] Moreover, this process would have partially blocked the drainage, thus inducing sedimentation on the Central Depression. This can explain the thick sedimentary filling of the Central Depression [*Farías et al.*, 2006b]. Because of the sedimentary filling, both the width of the valleys and the local base level were increased after burial of the preexisting river network beneath the Central Depression and eastern Coastal Cordillera. Thus the present-day morphology of the zone adjacent to the eastern Coastal Cordillera exhibits a landscape that appears to be more mature than the one observed in the Principal Cordillera (Figure 5).

4.2. High Elevated Peneplains in the Eastern Coastal Cordillera

[24] Between 33°S and 34°S, the eastern Coastal Cordillera rises up to ~2150 m asl (Figures 5 and 6a). To the south, maximum elevations decrease to <1000 m asl at 35°S (Figure 4). Highest summits of the Coastal Cordillera are flat-shaped, evidencing a relict continental surface of erosion [*Brüggen*, 1950; *Borde*, 1966]. The highest surfaces are mostly constructed on Cretaceous intrusive bodies; in turn, Mesozoic stratified sequences are better correlated with valley bottoms (Figure 2). Neither sediments nor volcanic deposits covering these surfaces have been reported.

[25] Several other surfaces at different elevations can be observed [*Borde*, 1966], however they are much smaller and less developed than the highest ones (Figure 4). Because of the absence of structures offsetting the different levels, their origin should be the base level fall. These surfaces have been interpreted as relicts of uplifted peneplains (peneplains in the sense of *Phillips* [2002]), i.e., they were constructed near its absolute base level [*Brüggen*, 1950; *Borde*, 1966]. Uplifted peneplains can be developed at high elevation if a barrier exists [*Babault et al.*, 2005]; in such model, deposition should occur. This is not observed on the eastern Coastal Cordillera, even though sediments could have been removed. Moreover, we consider unlikely the existence of a barrier because the surfaces are immediately to the east of Miocene-Pleistocene marine deposits and landforms. Thus peneplains should have developed close to the sea level. Considering that the sea level has not changed more than a few hundred meters [*Haq et al.*, 1987; *Miller et al.*, 2005], the elevation of the highest peneplains evidences surface

Figure 4. (a) Topographic swath profiles along the axis of each drainage basin. Swaths boxes are shown in Figure 3. Profile curves represent maximum, mean, and minimum elevations. Profiles are oriented N88°E, N90°E, N113°E, N114°E, N117°E (orthogonally oriented respect to the orogen strike), with swath width of 36, 80, 54, 40, and 38 km for the Aconcagua, Maipo, Cachapoal, Tinguiririca and Teno swaths, respectively; i1–i13 are the markers of incision (see Table 2). Solid lines on the maximum profiles are the correlation between the relicts of the peneplain surface. It can be observed that some vertical offset occurs, mainly along the San Ramón-Pocuro fault, including its southward prolongation (SRPF). (b) Comparison between maximum elevations. It can be noted that elevation diminishes gradually to the south. (c) Comparison between minimum elevations. In contrast to Figures 4a and 4b, the profiles in Figure 4c are horizontally fitted to the knickpoints situated close to eastern boundary of the Central Depression.

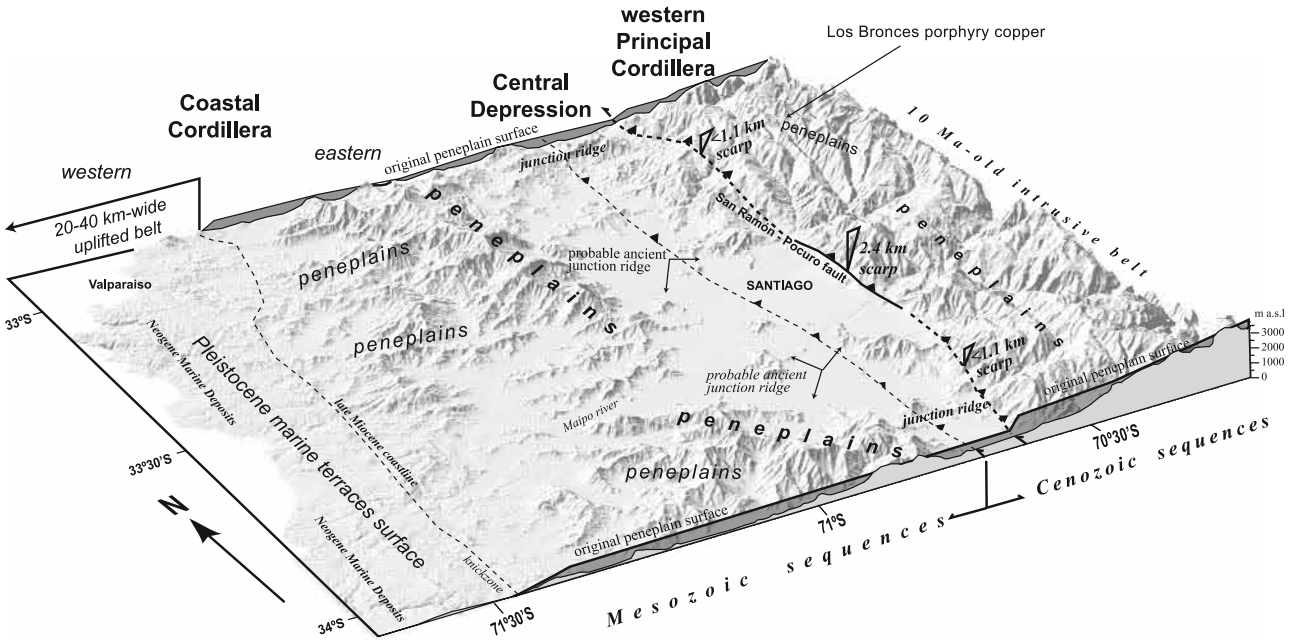

Figure 5. Three-dimensional view of the fore arc between 33°S and 34°S showing the evidence for surface uplift. The evidence consists of (1) relicts of peneplains surfaces and (2) emerged bathyal deposits along the coast. Junction ridges between the eastern Coastal Cordillera and the western Principal Cordillera (in addition to other features, see text for further explanation) evidence the erosive nature of the Central Depression. Relicts of peneplains in the eastern Principal Cordillera can be correlated with similar surfaces in the western Principal Cordillera. However, these surfaces are vertically offset by the San Ramón-Pocuro fault. Maximum upheaval related to this fault would be <1.1 at this zone. Thus ~1.3 km of the great scarp present immediately east of Santiago should be the result of erosion rather than tectonic activity along the cordilleran front.

uplift of 1.5–2.1 km at the latitude of Santiago, and ~1 km at 35°S.

[26] Because the highest peneplains are constructed on intrusive rocks and valleys are better correlated with stratified (mostly volcanic and volcanoclastic) rocks, preservation of high elevated peneplains would have been allowed by higher erosional resistance of intrusive rocks.

4.3. Relict Peneplains in the Principal Cordillera

[27] In the western Principal Cordillera, and in some places of the central Principal Cordillera, several flat erosional surfaces are located between 2600–3200 m asl (Figures 4, 5, 6b, 6c, and 6d). These surfaces were mainly constructed on the Farellones Formation, and their development probably was responsible for the destruction of the volcanic edifices of this unit. These surfaces gently dip to the west (1–3°) (Figure 4). Knickpoints as high as 1 km separate major valleys downstream from a less incised (<100 m) network upstream developed on the peneplain surfaces. Therefore the upstream part of the rivers corresponds to an initial network developed before the relative base level fall responsible for canyons incision. The incision that produced major valleys corresponds to either the uplift of the peneplain surface or the opening of a closed basin. The second alternative would require that the peneplains formed already at high elevation [*Babault et al.*, 2005] and the presence of a barrier responsible for the closure of the basin. This barrier could be the deformed belt along the westernmost Principal Cordillera (see Figures 2c and 5). However, peneplains extend to the Central Depression and eastern Coastal Cordillera forming some junctions between both ranges (Figures 4 and 5). Thus the existence of a closed basin is unlikely during the development of the peneplains. Therefore they would have been initially developed at low elevation.

[28] The peneplains present some vertical offsets. One of them can be related to the scarp of the San Ramón-Pocuro fault and its prolongation south of Santiago (Figures 3, 4, and 5). This scarp has its maximum height immediately east of Santiago (~2400 m high), where it is ~30 km long. In this zone, the base of the scarp is located along the eastern edge of the Central Depression. However, in the northern and southern parts of the Santiago depression, the base of the scarp is located in a westward prolongation of the western Principal Cordillera and the scarp is 700–1100 m high. In these places, the range extends to west forming junctions with the eastern Coastal Cordillera. Within the Santiago depression, some isolated hills seem to have also formed part of junctions (Figure 5). In fact, gravimetrical analyses show that these hills form ridges beneath the

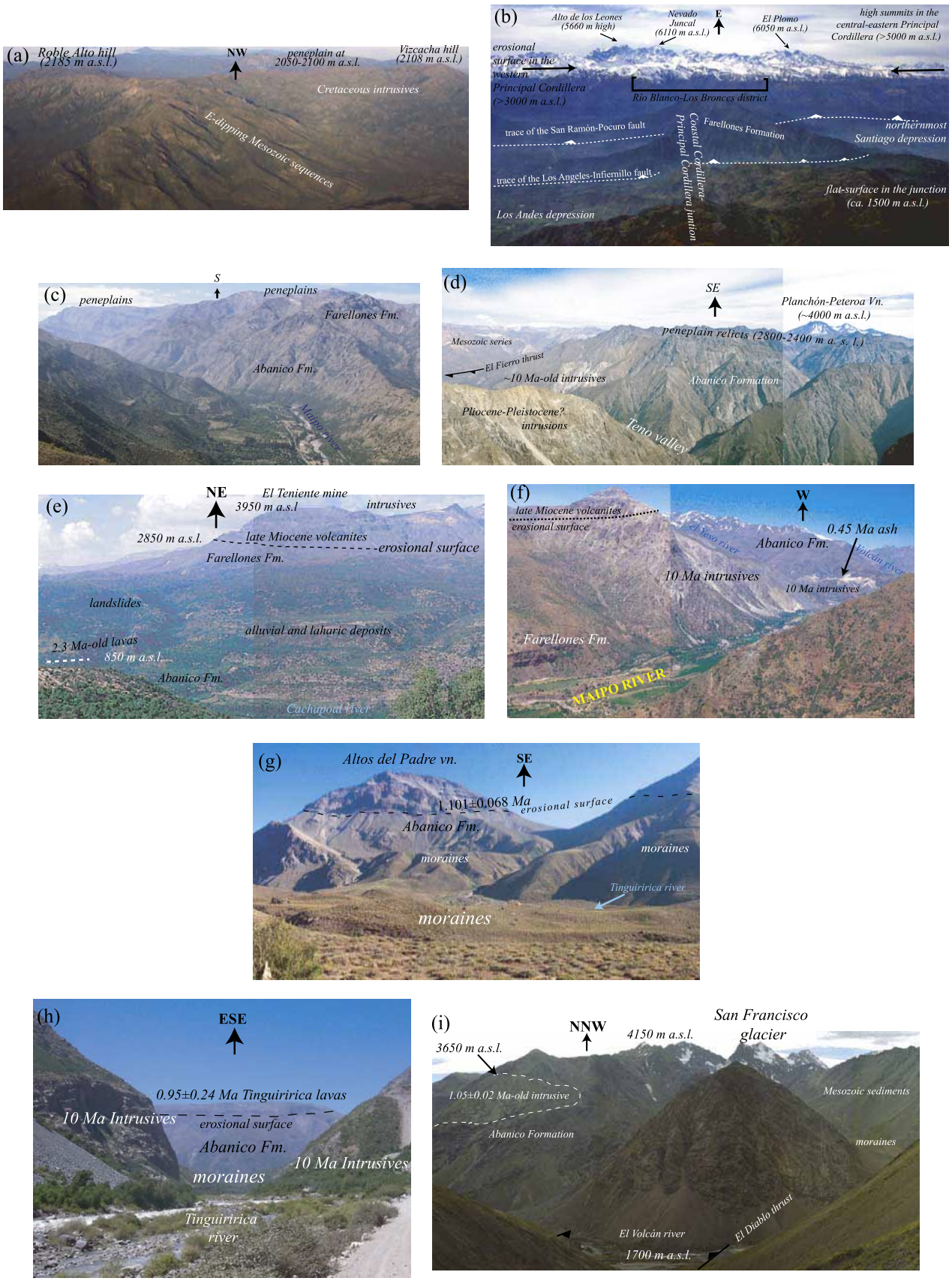
(a)
Roble Alto hill (2185 m a.s.l.)
NW
peneplain at 2050-2100 m a.s.l.
Vizcacha hill (2108 m a.s.l.)
Cretaceous intrusives
E-dipping Mesozoic sequences
(b)
Alto de los Leones (5660 m high)
Nevado Juncal (6110 m a.s.l.)
E
El Plomo (6050 m a.s.l.)
high summits in the central-eastern Principal Cordillera (>5000 m a.s.l.)
erosional surface in the western Principal Cordillera (>3000 m a.s.l.)
Río Blanco-Los Bronces district
trace of the San Ramón-Pocuro fault
Farellones Formation
northernmost Santiago depression
trace of the Los Angeles-Infiernillo fault
Coastal Cordillera-Principal Cordillera junction
flat-surface in the junction (ca. 1500 m a.s.l.)
Los Andes depression
(c)
S
peneplains
peneplains
Farellones Fm.
Abanico Fm.
Maipo river
(d)
SE
Planchón-Peteroa Vn. (~4000 m a.s.l.)
peneplain relicts (2800-2400 m a. s. l.)
Mesozoic series
El Fierro thrust
~10 Ma-old intrusives
Abanico Formation
Pliocene-Pleistocene? intrusions
Teno valley
(e)
NE
El Teniente mine
3950 m a.s.l
intrusives
2850 m a.s.l.
late Miocene volcanites
erosional surface
Farellones Fm.
landslides
alluvial and laharic deposits
2.3 Ma-old lavas
850 m a.s.l.
Abanico Fm.
Cachapoal river
(f)
late Miocene volcanites
erosional surface
W
el Yeso river
0.45 Ma ash
Abanico Fm.
Volcán river
10 Ma intrusives
10 Ma intrusives
Farellones Fm.
MAIPO RIVER
(g)
Altos del Padre vn.
SE
1.101±0.068 Ma
erosional surface
Abanico Fm.
moraines
moraines
Tinguiririca river
moraines
(h)
ESE
0.95±0.24 Ma Tinguiririca lavas
10 Ma Intrusives
erosional surface
Abanico Fm.
10 Ma Intrusives
moraines
Tinguiririca river
(i)
San Francisco glacier
NNW
4150 m a.s.l.
3650 m a.s.l.
1.05±0.02 Ma-old intrusive
Mesozoic sediments
Abanico Formation
moraines
El Volcán river
El Diablo thrust
1700 m a.s.l.

Figure 6

Table 2. Age of Incision Markers

	Long	Lat	Height, m asl	Rock	Age, Ma[a]	Method	Reference
i1	−70.7933	−34.746	650	basaltic andesite	1.25±0.03	Ar/Ar (WR)	this work[b]
i2	−70.7301	−34.7796	810	basaltic andesite	1.24±0.05	Ar/Ar (WR)	this work[b]
i3	−70.7358	−34.7321	916	basaltic andesite	1.06±0.03	Ar/Ar (WR)	this work[b]
i4	−70.6645	−34.7803	925	ignimbrite	0.803±0.133	Ar/Ar (fs)	this work[b]
i5	−70.5757	−34.2699	800	pyroxene andesite	1.8±0.4	K/Ar (WR)	*Charrier and Munizaga* [1979]
i6	−70.5516	−34.2266	900	pyroxene andesite	1.8±0.2	K/Ar (WR)	*Charrier and Munizaga* [1979]
i7	−70.5167	−34.216	880	pyroxene andesite	2.3±0.2	K/Ar (WR)	*Charrier and Munizaga* [1979]
i8	−70.3917	−34.1175	2850	dacitic dike	3.85±0.18	Ar/Ar (hbl)	*Maksaev et al.* [2004]
i9	−70.52	−34.8525	2800	basaltic andesite	0.95±0.24	K/Ar (WR)	*Arcos* [1987][c]
i10	−70.4691	−34.9816	2800	pyroxene andesite	1.101±0.068	K/Ar (WR)	*Arcos* [1987][c]
i11	−70.294	−33.0025	3200	dacitic dike	5.88±0.27	U/PB zrn maximum age	*Deckart et al.* [2005]
					4.55±0.18	U/PB Zrn minimum age	*Deckart et al.* [2005]
					4.916±0.091	U/PB zrn mean weighted age	*Deckart et al.* [2005]
i12	−70.0991	−33.7716	3650	biotite dacite	1.20±0.19	Ar/Ar plateau (hbl)	*Baeza* [1999][d]
					1.05±0.02	Ar/Ar plateau (bt)	*Baeza* [1999][d]
i13	−70.2	−33.7974	1500	ash deposit	0.45±0.06	zircon fission track	*Stern et al.* [1984]

[a]All K-Ar and Ar/Ar ages with 2σ error. Zircon fission track age with 1σ. WR, whole rock; bt, biotite; fs, feldspar; hbl, hornblende; zrn, zircon.
[b]See auxiliary material section S1 for details.
[c]Datation performed at the Laboratory of Geochronology, University of California, Berkeley.
[d]Datation performed at the Department of Geological Science, University of California, Santa Barbara.

sedimentary infill of the Central Depression [*Araneda et al.*, 2000]. According to these data, these ridges correspond to interfluves of a buried drainage network, which evidence the erosive nature of the Central Depression. Farther south at 34°35′S, the Principal Cordillera also joins the Coastal Cordillera (Figure 4), and the scarp is less sharp and lower than in Santiago (600–800 m high).

[29] Because the scarp height shows local variations, its height cannot be completely considered as the result of fault activity (see Figures 4 and 5). Therefore the upheaval resulted from faulting can be only estimated from the offset of the peneplain surface. Thus faulting would have produced a relative uplift of 0.7–1.1 km at the latitude of Santiago and 0.6–0.8 km at 34°30′S (Figure 4). The rest of the scarp height should then be the result of differential erosion in response to surface uplift [*Borde*, 1966; *Farías et al.*, 2006b].

5. Erosional Response of the Landscape to Surface Uplift

5.1. Timing of Incision in the Principal Cordillera

[30] Close to the Río Blanco–Los Bronces porphyry-copper deposit (western Principal Cordillera at ∼33°S), the La Copa volcanic-porphyric complex has sensitive high-resolution ion microprobe (SHRIMP) $^{238}U/^{206}Pb$ zircon ages between 4.55 ± 0.18 and 5.88 ± 0.27 Ma (4.92 ± 0.09 Ma calculated weighted mean age, Table 2) [*Deckart et al.*, 2005]. The top of the unit is at ∼3900 m asl and approximately coincides with the elevation of the peneplain surface at this place (Figures 5 and 6b). The dated sample was collected at ∼3200 m asl, close to the lowest altitude observed for the contact between this complex and the host rock that corresponds to middle Miocene intrusives [see *Deckart et al.*, 2005, and references therein]. At the present, the Aconcagua river is ∼2 km below this contact. Thus incision has mainly occurred after ∼5 Ma in the western edge of the Principal Cordillera at 33°S.

[31] About 30 km upstream from the Central Depression near the El Teniente porphyry copper (western Principal Cordillera in the Cachapoal basin), lavas and plutons reach altitudes between 2850 and 3950 m asl (Figure 6e). The base of the volcanic and intrusive bodies is ∼2 km above the present-day thalweg (sample i8 in Table 2). This base corresponds to a flat discordance that can be correlated, based on its elevation, with the peneplain surface in the western Principal Cordillera. These units have a youngest $^{40}Ar/^{39}Ar$ age of 3.85 ± 0.18 Ma [*Maksaev et al.*, 2004]. In addition, 150 m above the valley bottom of the Cachapoal

Figure 6. Pictures of the evidence for surface uplift in the study region. (a) View to one of the highest peneplain relicts in the eastern Coastal Cordillera, northwest of Santiago. (b) View to the Principal Cordillera from the Coastal Cordillera in the ridge junction located north of Santiago. (c) View to the peneplain relicts in the western Principal Cordillera in the Maipo river. (d) View to peneplain relicts in the western Principal Cordillera, south of the Teno valley. (e) Incision markers in the Cachapoal valley near the El Teniente copper mine (western Principal Cordilelra). (f) 0.45 Ma old ash deposit over the ∼10 Ma old intrusives in the Maipo river. (g) The Altos del Padre volcanic complex in the Tinguiririca valley. (h) Tinguiririca lavas close to the ∼10 Ma old intrusive belt. (i) Approximately 1.05 Ma intrusive in the Volcán valley (central Principal Cordillera in the Maipo basin).

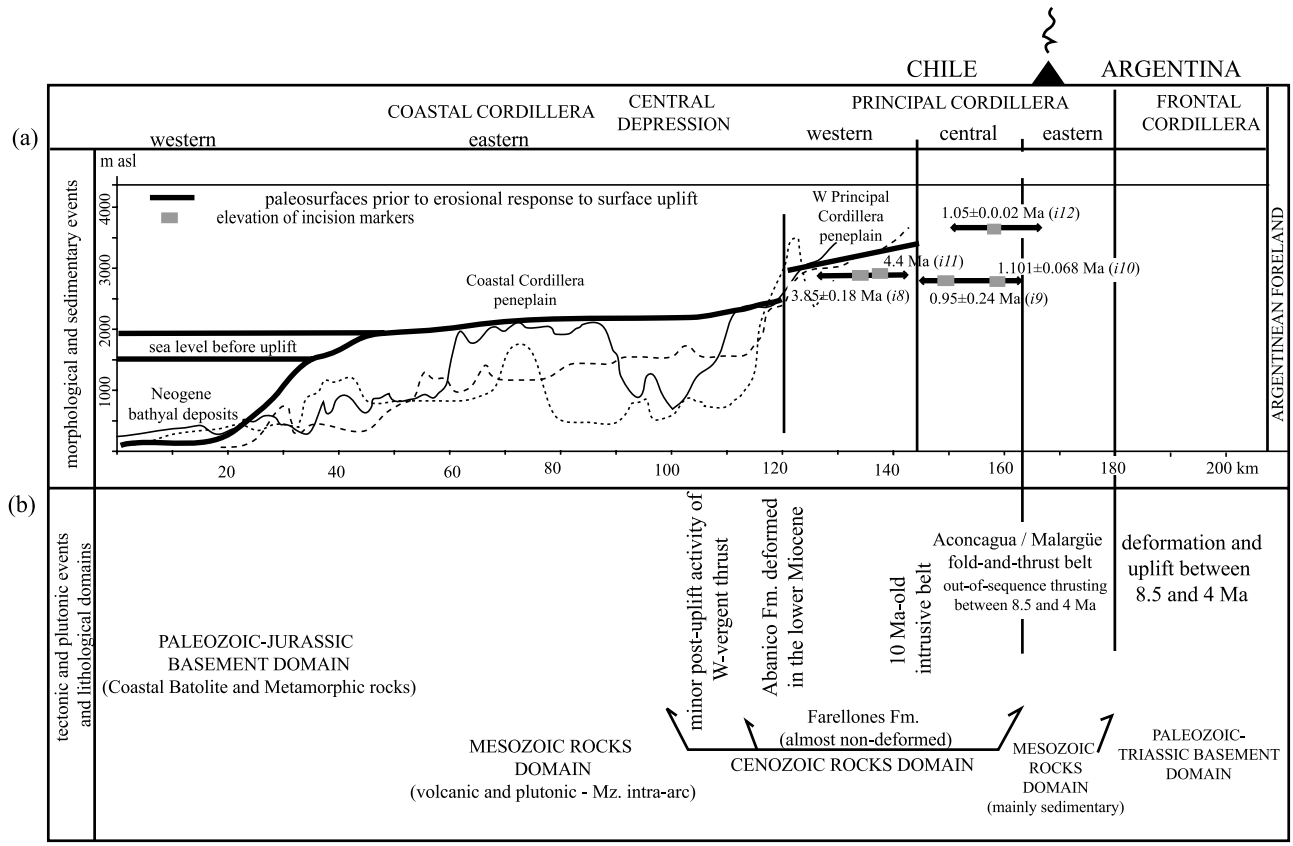

Figure 7. Summary of (a) evidence for regional surface uplift and (b) main tectonic events in the study region. Topographic profiles are smoothed and correspond to those shown for the Maipo swath in Figure 4. The tectonics events in Figure 7b correspond to those that occurred at the latitude of Santiago. The 0 km is approximately the present-day coastline. Limits of morphostructural units, volcanic arc, and international border are approximated.

river (at ~880 m asl), *Charrier and Munizaga* [1979] reported lava deposits with K/Ar ages of 2.3 ± 0.2 Ma (oldest age) and 1.8 ± 0.4 Ma (youngest age) (Figure 6e). Therefore incision mostly occurred between 3.85 and 2.3 Ma at this place.

[32] About 10–15 km upstream from the Central Depression in the Tinguiririca valley, ~1.1 Ma old lavas (i1–i3) are located ~150 m above the thalweg. About 15–20 km upward from there, these deposits sealed a paleovalley situated 200–250 m above the river (i4 in Table 2). Upstream from the ~10 Ma old intrusive belt, the 1.1–0.9 Ma old Altos del Padre volcanic complex (i9–i10 in Table 2) [*Arcos*, 1987] settled on a flat discordance above the Abanico Formation (Figures 6g and 6h). The base of this unit is at 2850–2750 m asl (1150 m and 1450 m above the Tinguiririca and Teno rivers, respectively). Hence mean incision has occurred at rate of 1.3–1.5 mm a^{-1} since ~1.1 Ma, similar to the incision rate calculated in the western Principal Cordillera in the Cachapoal basin, even though incision was older there.

[33] In the eastern edge of the central Principal Cordillera in the Volcán river valley (Maipo river basin), a 1.05–1.20 Ma old pluton (sample i12 in Table 2) intrudes the Abanico Formation [*Baeza*, 1999]. The roof of this body is at 3650 m asl, i.e., almost 2 km above the valley bottom and ~500 m below the top of the hillslope (Figure 6i). In addition, about 150 m above the river, an ash deposit covering a thin layer of fluvial deposits emplaced over the 10 Ma old intrusive belt has an age of 0.45 ± 0.06 Ma [*Stern et al.*, 1984] (sample i13 in Table 2, see Figure 6f). Therefore 2.4 km of incision occurred between 1.1 and 0.45 Ma at this place (~2.8 mm a^{-1} of mean incision rate).

[34] Figure 7 sums up the data evidencing surface uplift. Incision in the eastern Coastal Cordillera and Central Depression has been ~1.8 km, at the latitude of Santiago, and ~0.8 km, at 35°S. Incision has been 2–2.5 km in the western Principal Cordillera, and between 1.5 (at 34°30′S) and 2.5 km (at 33°45′S) in the central Principal Cordillera and eastern Principal Cordillera. Therefore minimum surface uplift should be smaller than or equal to the incision in each region. Because at each location the incision was very rapid, we infer that the uplift would have also occurred very rapidly in >2 Ma.

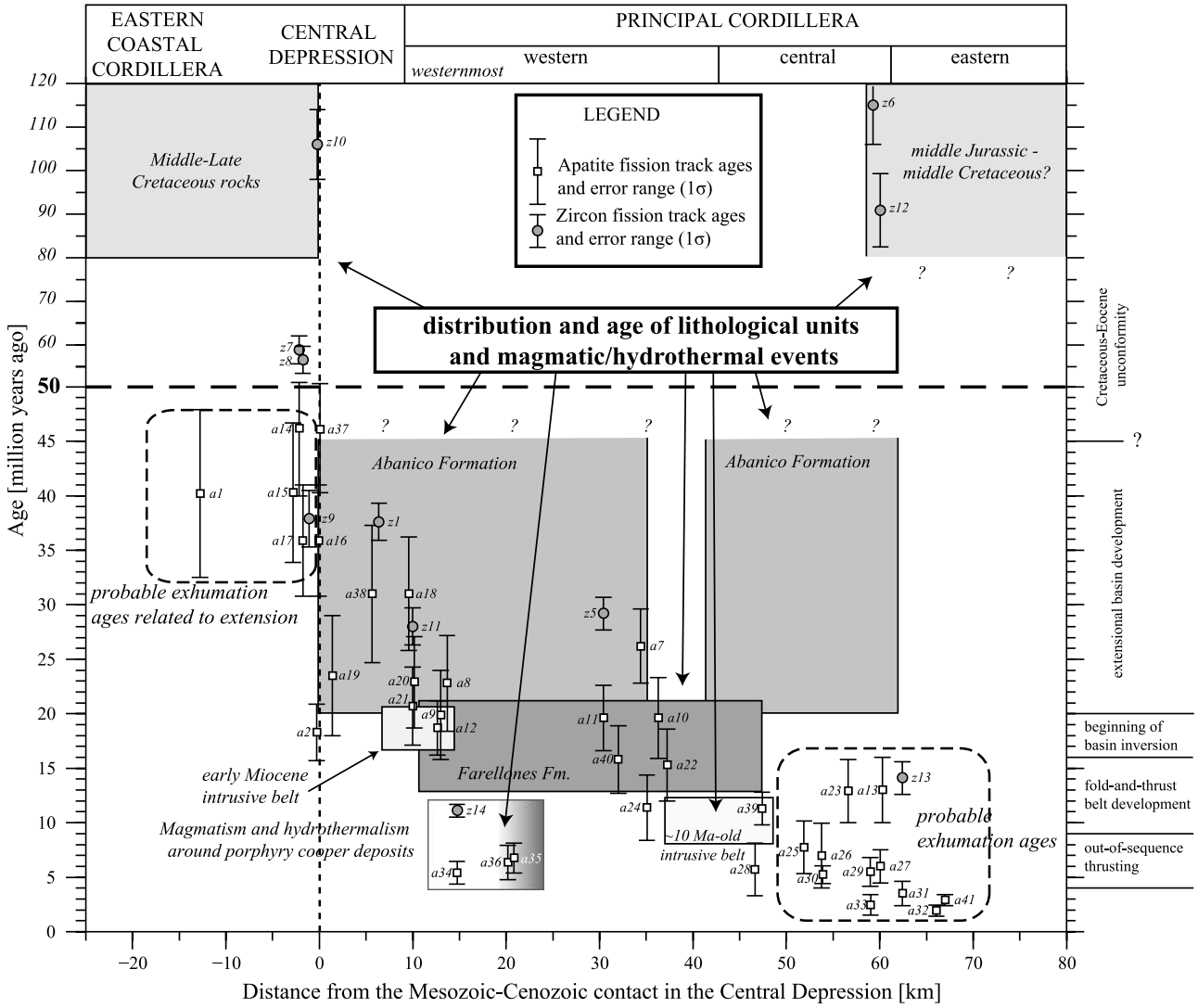

Figure 8. Fission track ages projected on profiles perpendicular to the orogen strike. The 0 km is as in Figure 4. Distribution and age of lithological units and magmatic/hydrothermal events permit their correlation with some fission track ages and interpret exhumation (see text). Age range for the Abanico Formation is after *Gana and Wall* [1997], *Vergara et al.* [1999], *Charrier et al.* [2002], *Fuentes et al.* [2002], and *Fock et al.* [2005]; for the Farellones Formation is after *Vergara and Drake* [1978], *Beccar et al.* [1986], *Aguirre et al.* [2000], and *Fuentes et al.* [2002]; for the magmatic and hydrothermal activity in porphyry copper systems is after *Vergara and Drake* [1978], *Maksaev et al.* [2004], and *Deckart et al.* [2005]; and for the ~10 Ma old intrusive belt is after *Vergara and Drake* [1978], *Kurtz et al.* [1997], and *Cornejo and Mahood* [1997].

5.2. Fission Track Ages

[35] Figure 8 shows the 41 apatite fission track (AFT) and the 14 zircon fission track (ZFT) ages obtained in this study (see Figure 3 for sample location and auxiliary material[1] section S2 for details).[1] Most of the samples were collected near the valley bottoms. Data are plotted as a function of the distance from the Mesozoic-Cenozoic contact in the Central Depression (see Figures 2 and 3 for the location of this contact). In the central Principal Cordillera and eastern Principal Cordillera, AFT ages range between 1.4 and 10 Ma. Because these ages are much younger than the host rocks (Mesozoic and Eocene–lower Miocene), they correspond either to exhumation or cooling after resetting by postdepositional magmatic activity. It is likely that the ages that fall close to 10 Ma correspond to cooling ages after the heating produced by the emplacement of the ~10 Ma old intrusive belt. It is unlikely that the youngest ages are related to such a process because the youngest intrusive bodies are very small in comparison with the 10 Ma old belt. For example, the ~1.2 Ma old pluton

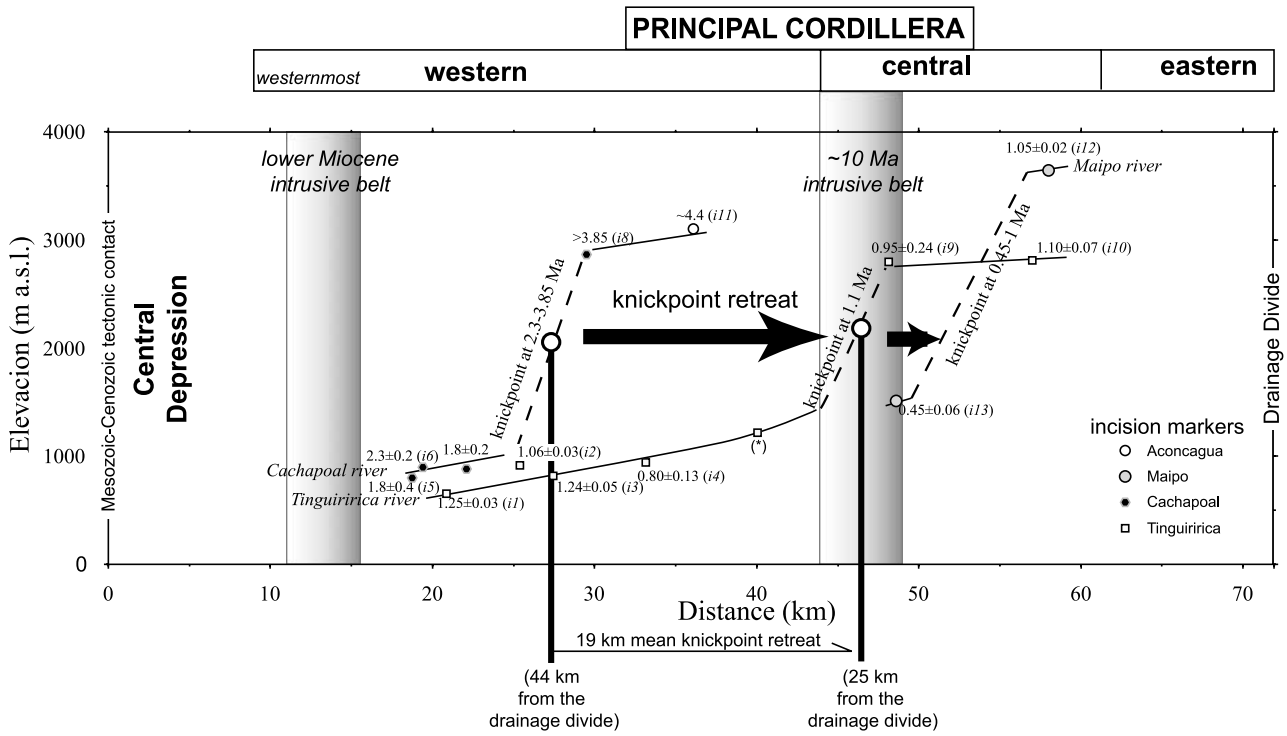

Figure 9. Analysis of incision markers and knickpoint retreat in the Tinguiririca and Cachapoal basins. Markers are plotted along transect perpendicular to the orogen strike. On the basis of the markers in the Cachapoal river valley, the mean position of the knickpoint between 3.85 and 2.3 Ma was 44 km downstream from the drainage divide, while in the Tinguiririca river, the knickpoint at 1.1 Ma was 25 km downstream from the drainage divide. Considering the mean distance between both knickpoints, the retreat celerity ranges between 6.5 and 19 mm a^{-1} with a central value of 9.6 mm a^{-1} (Table 3). The markers of the rest of the basins are also displayed as reference. The star shows the prolongation of base of the lava layer observed downstream. Ages are in millions years ago.

located at the Volcán valley extents over less than 1 km^2. Neglecting the ~10 Ma old AFT ages, the main population of AFT ages ranges from 1 to 5 Ma. Therefore AFT ages in the central Principal Cordillera and eastern Principal Cordillera could represent exhumation rather than a magmatic/hydrothermal heating and cooling effect.

[36] In turn, AFT ages obtained in the western Principal Cordillera fit well with depositional ages of the Abanico and Farellones formation, except near the porphyry copper deposits (Figure 8). We suspect that youngest cooling ages close to these deposits mark the magmatic and hydrothermal activity there. In fact, the youngest U/Th-He age of 2.4 Ma obtained by *McInnes et al.* [2005] close to the El Teniente mine is very similar to the oldest age obtained for the lava deposit close to the thalweg in the Cachapoal river (2.3 ± 0.2 Ma). This situation is in agreement with a magmatic heating and cooling effect rather than exhumation. On the other hand, the similarity between the AFT and depositional ages obtained in the western Principal Cordillera shows that rocks were not heated above 110–125°C.

[37] In summary, fission track ages suggest that exhumation occurred mostly after 5 Ma in the central and eastern Principal Cordillera, which is consistent with the age of the main event of incision. On the other hand, exhumation in the western Principal Cordillera, eastern Coastal Cordillera, and Central Depression has not been large enough to expose rocks that underwent apatite fission track resetting during the Neogene. In spite of the good correlation between larger incision in the central and eastern Principal Cordillera and the AFT ages, the presence of <5 Ma old plutons at this place can alternatively explain the younger cooling ages.

5.3. Estimating Celerities and Shape of Upstream Propagation of the Erosion

[38] On the basis of the data presented above, it is possible to estimate where knickpoints were located during the upward propagation of the erosion. Particularly, three knickpoint positions and their respective ages can be directly interpreted from these data. The first one can be inferred in the central Principal Cordillera along the Maipo basin, where the knickpoint crossed between 1.2 and 0.45 Ma (Figure 9). Likewise, the knickpoint crossed the zone close to the El Teniente mine along the Cachapoal basin between 3.85 and 2.3 Ma. The position and age of the knickpoints in these basins, however, is only roughly estimated on the basis of this methodology.

Table 3. Calculation of Knickpoint Celerity[a]

Parameter	Value	Description	Reference
		Calculation of the Erodability Constant K	
b	44,000 m	distance of 3.85–2.3 Ma old knickpoint from the drainage divide	see Figure 9
a	25,000 m	distance of the 1.1 Ma old knickpoint from the drainage divide	see Figure 9
h	1.76	reciprocal of Hack's law	values obtained in section 3 (Table 1)
k_a	6.12 $m^{0.24}$	constant of Hack's law	
m	0.5	adimensional exponent of the stream power law	
n	1	adimensional exponent of the stream power law	
C_{ba}	0.0065 m a^{-1}	minimum mean speed between both knickpoints	values obtained in section 5.3 (see Figure 9)
	0.0190 m a^{-1}	maximum mean speed between both knickpoints	
	0.0096 m a^{-1}[b]	central mean speed between both knickpoints	
K	2.73×10^{-7} a^{-1} (minimum)	erodability constant of the stream power law	calculated from equation (A7)
	7.97×10^{-7} a^{-1} (maximum)		
	4.03×10^{-7} a^{-1} (central)[b]		
		Calculation of the Onset of the Surface Uplift	
d	140,000 m	distance from paleocoast up to the drainage divide	
e	44,000 m	distance of the 3.85–2.3 Ma old knickpoint from the drainage divide	
C_{de}	0.01446 m a^{-1}	minimum mean speed between d and e	calculated from equation (A6)
	0.04226 m a^{-1}	maximum mean speed between d and e	
	0.02135 m a^{-1} [b]	central mean speed between d and e	
$T = (d\text{-}e)/C_{de}$	2.27 Ma (minimum)	timing for arrival to the Principal Cordillera	
	6.64 Ma (maximum)		
	4.50 Ma (central)[b]		
T_0	4.57 Ma (minimum)	age of the onset of surface uplift	
	10.49 Ma (maximum)		
	7.58 Ma (central)[b]		

[a]Calculations were made using the equations in Appendix A.
[b]Central value obtained from the mean age of knickpoint pass in the Cachapoal river between 2.3 and 3.85 Ma (3.075 Ma) and subsequent calculations.

[39] In turn, the ~1.1 Ma old lavas deposited in the Tinguiririca valley mark very well the position of the knickpoint at that time. The lavas are situated very near the valley bottom in the western Principal Cordillera. In turn, the bedrock where the lavas were deposited increases its elevation up to ~1.5 km above the valley bottom near the ~10 Ma old intrusive belt (Figure 9). Moreover, the geometry of the thalweg where the lavas were deposited (Figure 9) can be interpreted as the result of knickpoint retreat under a parallel-retreat model (see Figure 1).

[40] Morphometric parameters between the Tinguiririca and Cachapoal basins (Hack's law parameters, see Table 1) can be considered comparable. However, the much larger drainage area of the Maipo basin does not allow a quantitative comparison with the other basins. Because of this, we made a quantitative analysis of the knickpoint positions and timing in the Cachapoal and Tinguiririca valleys (Figure 9).

[41] This procedure shows that the knickpoint at 2.3–3.85 Ma was situated 44 km from the drainage divide, and that at 1.1 Ma, it was situated 19 km upward (25 km from the drainage divide, see Table 3). Using these values, the knickpoint retreat celerity between these two points ranges between 6.5 and 19 mm a^{-1} with a central value of 9.6 mm a^{-1}. It is necessary to point out that knickpoint celerity is a mean value that is only valid for the segment between two knickpoint locations; in fact, celerity should vary with drainage area (see Appendix A for further explanation about the stream power model). Thus it is not valid to use directly this value to estimate the age of the onset of knickpoint retreat.

[42] In order to estimate this age, we used a stream power law model for detachment-limited systems based on the work by *Whipple and Tucker* [1999] (see Appendix A). The stream power law relates the erosion rate to the drainage area A (as proxy for discharge) and the slope S (see equation (A1)). We assumed values for the nondimensional constants n and m of the stream power law to be 1 and 0.5, respectively. We used $n = 1$ because this value is consistent with the observed parallel retreat [cf. *Tucker and Whipple*, 2002]. Moreover, $m = 0.5$ is consistent with predicted values of the m/n ratio, which commonly fall into a narrow range near 0.5 [see *Whipple and Tucker*, 1999, and references therein]. We also used the parameters of Hack's law previously calculated (Table 1). On the basis of these assumptions, we determined an erodability constant K

Table 4. Summary of Some Knickpoint Retreat Speed Estimates[a]

Location	Knickpoint Retreat Rate, mm a^{-1}	Timescale, years	Reference
Dead Sea basin	0.25–0.50	10^6–10^7	*Haviv et al.* [2003]
Hawaii	0.5–2	10^6	*Seidl et al.* [1994]
SE Australia	~2.0	10^7–10^8	*Nott et al.* [1996]
Northern Chile	~10	10^6–10^7	*Schlunegger et al.* [2006]
Utah	~10	10^3–10^4	*Phillips et al.* [2004]
Andes of central Chile	6.5–19, Principal Cordillera 14.5–42.3, Coastal Cordillera and Central Depression	10^6–10^7	this work
San Jacinto mountains, California	12–44	10^6	*Dorsey and Roering* [2006]
Jalisco, Mexico	36	10^6	*Righter* [1997]
SE Spain	200	10^4–10^5	*Mather et al.* [2002]
Costa Rica arc	200–250	10^6	*Marshall et al.* [2003]
Yalobusha river, Mississippi basin	5.4×10^2 to 1.55×10^4	> 4	*Simon and Thomas* [2002]
Homichitto river, Mississippi basin	1.5×10^4 to 9.4×10^5	60	*Daniels* [2002]

[a]Note that sites are in descending order according to their knickpoint retreat celerity.

ranging between 2.7×10^{-7} a^{-1} and 8.0×10^{-7} a^{-1} (see Appendix A and Table 3).

[43] These values allow us to compute a mean celerity function depending on the downstream distance (see Appendix A). Integrating the celerity, the model suggests that knickpoint retreat began at 10.5–4.6 Ma if it started in the western edge of the eastern Coastal Cordillera (expected coastline at this time), and at 5.6–2.9 if it started in the western edge of the Principal Cordillera (western scarp of the mountain belt, namely, the San Ramón-Pocuro fault and its southward prolongation). These ages correspond to retreat celerities ranging between 10 and 40 mm a^{-1}, which can be considered as slow-to-mean values (see Table 4).

6. Discussion

[44] The relicts of peneplains located near the summits of the eastern Coastal Cordillera and in the Principal Cordillera show that an uplift occurred at a regional scale but not necessary at the same time everywhere. Furthermore, emerged marine sediments near the present-day coastline (western Coastal Cordillera) show that this area has been also considerably uplifted. Next, we address the following questions that our data cannot solve directly: (1) Did the peneplains of the eastern Coastal Cordillera and western Principal Cordillera correspond the same surface? (2) Was the uplift in the continental margin contemporaneous everywhere? (3) When did it occur? (4) Which were the controlling mechanisms for regional uplift in this region?

[45] First, we propose to correlate the peneplains of the eastern Coastal Cordillera with those of the western Principal Cordillera that are facing each other. The main problem of this correlation is the lack of an age for the peneplains of the eastern Coastal Cordillera. There, fission track ages have provided Eocene ages, which coincide with the beginning of the extension that led to the development of the Abanico basin. It is unlikely that low-temperature thermochronometers show younger ages because more than 10 km of exhumation would be required to record exhumation because of the low geothermal gradient estimated for this area [e.g., *Oleskevich et al.*, 1999; *Yáñez and Cembrano*, 2004]. The absence of volcanic and sedimentary cover on the surfaces makes particularly difficult to date these peneplains. Furthermore, because the primary surfaces are degraded, cosmogenic dating would reflect younger ages than the peneplanation event. In spite of these problems, it is likely that two offset peneplain surfaces facing each other would have belonged to the same surface because both the most prominent offset correlates with an active fault (San Ramón-Pocuro fault and its southward prolongation) [*Rauld et al.*, 2006] and the surfaces present a great morphological similitude.

[46] As previously mentioned, the San Ramón-Pocuro fault (and its southward prolongation) would have produced no more than 1.1 km of relative upheaval on the eastern block (western Principal Cordillera) at the latitude of Santiago, and no more than 800 m at 35°S. Because the incision in the western Principal Cordillera at 34°S was more than 2 km, the Principal Cordillera and eastern Coastal Cordillera should have been uplifted during the same event with a greater offset (30% more) east of the San Ramón-Pocuro fault, including its southward prolongation. Most of this differential uplift probably occurred during the main regional uplift event because only ~150 m of incision occurred in the main rivers of the western Principal Cordillera after 2.3 Ma. If effectively the surfaces observed in the eastern Coastal Cordillera and western Principal Cordillera corresponded to the same peneplains, the uplift would have began at 10.5–4.6 Ma according to our erosion model.

[47] The emergence of marine deposits in the western Coastal Cordillera occurred between 4.4 and 2.7 Ma. The similitude between the youngest extreme for the onset of knickpoint retreat from the western edge of the eastern Coastal Cordillera (4.6 Ma), and the oldest extreme for the

emergence of marine deposit in the western Coastal Cordillera (4.4 Ma) suggests that regional and sudden uplift occurred shortly before 4 Ma. This model would have affected the entire Coastal Cordillera and Principal Cordillera (model 1, Figure 10a).

[48] However, we propose an alternative model based on complementary evidence and the synchronism with major geodynamic events in this region (model 2, Figure 10b). This model suggests that the western Coastal Cordillera and the offshore fore arc were uplifted after the eastern Coastal Cordillera and Principal Cordillera and that the uplift magnitude was different in each zone. We base this proposition on the following facts. In the eastern Coastal Cordillera, the relicts of peneplains decrease in elevation from 2100 at 33°S to <1000 m asl at 35°S. Although the peneplain surface could have had variable altitudes before uplift, this strong decrease indicates that the uplift also decreased to the south. The situation described above seems to be supported by the fact that the elevation of the western Principal Cordillera decreases southward approximately at the same rate as that of the eastern Coastal Cordillera (Figure 4). This feature is also supported by an approximately similar southward rate of reduction of the crustal thickness [see *Tassara et al.*, 2006]. In turn, the magnitude of uplift of the western Coastal Cordillera has been showed to be nearly the same from 33°–34° to 45° [*Encinas et al.*, 2007; *Finger et al.*, 2007; *Melnick and Echtler*, 2006]. This suggests the existence of a fault system separating the western from the eastern Coastal Cordillera. Such a fault system has been described by *Melnick et al.* [2006] at 37–38°S and can be inferred by the location of bedrock rivers along the mainstreams near the coast (see Figure 5). Concerning the onset of uplift in both parts (i.e., western Coastal Cordillera and eastern Coastal Cordillera–western Principal Cordillera), if we consider a 3.4 Ma age (mean age) for the emergence of the bathyal deposits and a 7.6 Ma age (central age, see Table 3) for the onset of knickpoint retreat, it is possible to conclude that the western Coastal Cordillera was uplifted after the rest of the Andes of central Chile. However, this is a somewhat weak argument considering the uncertainty on the incision model used to estimate the erosion onset.

[49] In spite of this, three other major events in this region occurred between 10 and 4 Ma: (1) at ~10 Ma the southern edge of the flat slab subduction zone reached its present-day location at ~33°S [*Yáñez et al.*, 2001] (the southern boundary of the flat subduction is at 33°S, namely, the north boundary of the study area), (2) the uplift of the Frontal Cordillera and the development of out-of-sequence thrusts in the central eastern Principal Cordillera, and (3) a high subsidence of the western Coastal Cordillera and the offshore fore arc [*Encinas et al.*, 2007; *Finger et al.*, 2007].

[50] Some works have related the flattening of the slab to the reactivation of high-angle basement structures, which resulted in the uplift of the Frontal Cordillera and Precordillera, and in the subsequent activity of out-of-sequence thrusts in the Principal Cordillera [e.g., *Ramos et al.*, 2002; *Giambiagi and Ramos*, 2002]. The out-of-sequence thrusting event in the central eastern Principal Cordillera lasted until ~4 Ma. At this time, shortening migrated farther east to the foreland. In fact, present-day deformation within the Principal Cordillera is mainly related to strike-slip kinematics according to the Harvard CMT focal mechanism for shallow earthquakes M>5 recorded during the last three decades [*Farías et al.*, 2006a]. We propose that the forelandward migration of shortening would have occurred because of the large elevation reached by the mountain belt after the main surface uplift event (Figure 10b); that is, the increase in vertical stress would have resulted large enough to prevent contraction within the mountain belt and to produce the migration of the shortening to the lowlands (see, for example, the model of *Dalmayrac and Molnar* [1981]). This migration would have been also favored by a decreasing convergence rate at this time [*Somoza*, 1998] that would have led to a decrease in the horizontal stress. Therefore elevation reached by the mountain belt at ~4 Ma would not differ too much from its current elevation and is, thus, consistent with great uplift at 10–4 Ma.

[51] Between 10 and 4 Ma, the western Coastal Cordillera was subsiding [*Finger et al.*, 2007; *Encinas et al.*, 2007]. *Encinas et al.* [2007] considered that the only reliable process that could produce this subsidence is the tectonic erosion of the continental margin. This process occurring in the coastal offshore fore arc could be consistent with contemporaneous uplift of the rest of the Andes in the study region (see the model of *Lamb and Davis* [2003]). On the other hand, *Melnick and Echtler* [2006] proposed that uplift of the bathyal deposits would have been the result of frontal accretion and subduction of water-rich material due to an increase on sediment flux incoming to the trench (Figure 10b). Melnick and Echtler proposed that the onset of glacial denudation in the already uplifted high Andes would have propitiated this process. We consider likely that fluvial erosion of the mountain belt in response to the surface uplift could have also contributed to increase the sediment flux incoming to the trench (Figure 10b). This is because knickpoints arriving in the western Principal Cordillera at 3.8–2.3 Ma would have increased the rate of sedimentary production, which is consistent with the ages for the onset of the uplift of the western Coastal Cordillera and the offshore fore arc.

Figure 10. Models for surface uplift. (a) Model 1. This model implies that uplift occurred shortly before 4 Ma. Uplift in this model affected simultaneously the offshore fore arc, Coastal Cordillera and Principal Cordillera. (b) Model 2. This model implies that uplift occurred in the eastern Coastal Cordillera and Principal Cordillera, while the offshore fore arc and western Coastal Cordillera subsided at this time. Following to the model proposed by *Melnick and Etchler* [2006], in this scenery the erosion in the already uplifted Principal Cordillera and eastern Coastal Cordillera would have increased the sediment flux into the trench, thus inducing the uplift of the offshore fore arc and western Coastal Cordillera after 4 Ma.

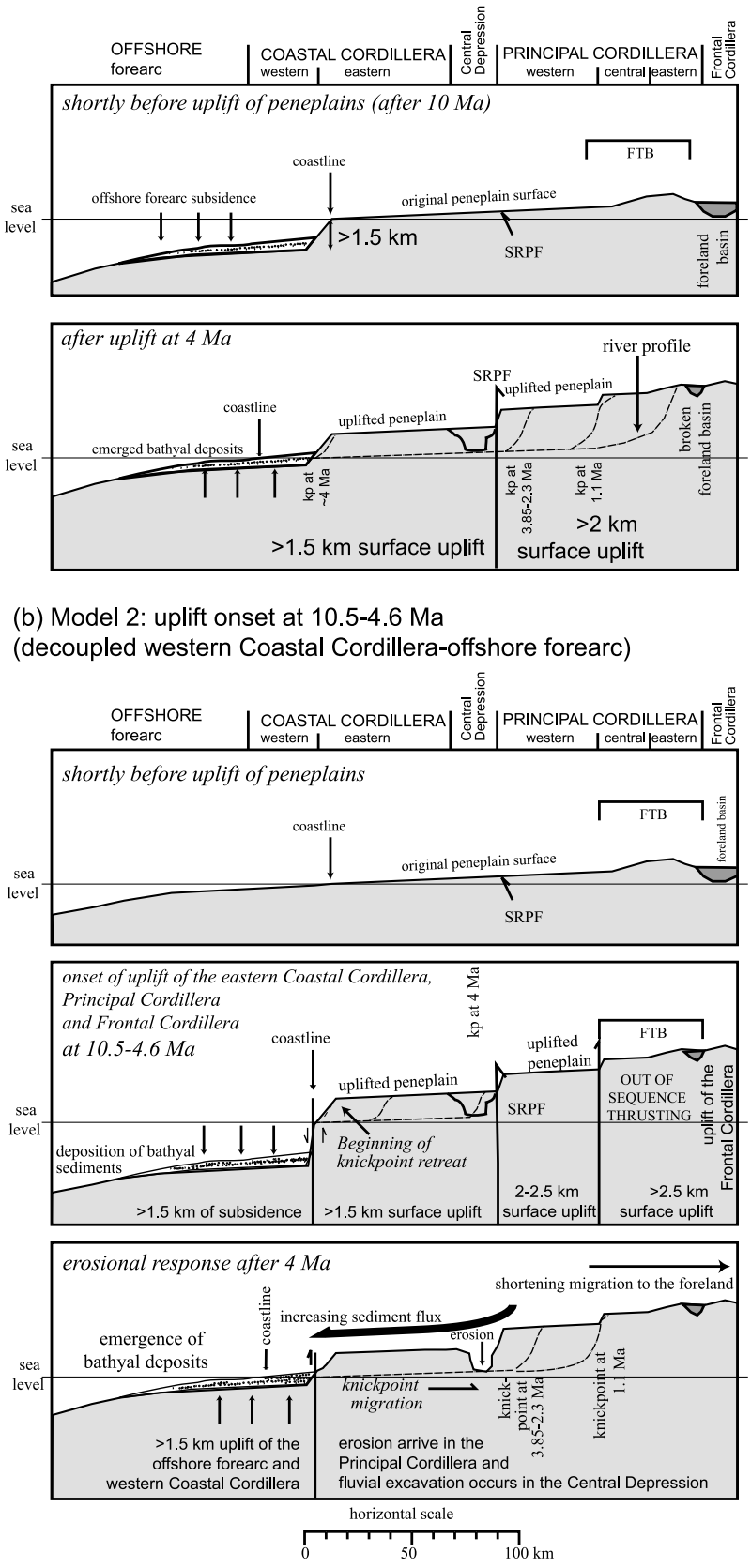
(a) Model 1: uplift at ~4 Ma (coupled Coastal Cordillera)
OFFSHORE forearc
COASTAL CORDILLERA western eastern
Central Depression
PRINCIPAL CORDILLERA western central eastern
Frontal Cordillera
shortly before uplift of peneplains (after 10 Ma)
FTB
coastline
offshore forearc subsidence
original peneplain surface
sea level
>1.5 km
SRPF
foreland basin
after uplift at 4 Ma
river profile
SRPF
uplifted peneplain
coastline
uplifted peneplain
emerged bathyal deposits
sea level
kp at ~4 Ma
kp at 3.85-2.3 Ma
kp at 1.1 Ma
broken foreland basin
>1.5 km surface uplift
>2 km surface uplift
(b) Model 2: uplift onset at 10.5-4.6 Ma
(decoupled western Coastal Cordillera-offshore forearc)
OFFSHORE forearc
COASTAL CORDILLERA western eastern
Central Depression
PRINCIPAL CORDILLERA western central eastern
Frontal Cordillera
shortly before uplift of peneplains
FTB
coastline
original peneplain surface
foreland basin
sea level
SRPF
onset of uplift of the eastern Coastal Cordillera, Principal Cordillera and Frontal Cordillera at 10.5-4.6 Ma
kp at 4 Ma
coastline
uplifted peneplain
uplifted peneplain
FTB
OUT OF SEQUENCE THRUSTING
SRPF
uplift of the Frontal Cordillera
sea level
deposition of bathyal sediments
Beginning of knickpoint retreat
>1.5 km of subsidence
>1.5 km surface uplift
2-2.5 km surface uplift
>2.5 km surface uplift
erosional response after 4 Ma
shortening migration to the foreland
coastline
increasing sediment flux
erosion
emergence of bathyal deposits
sea level
knickpoint migration
knick-point at 3.85-2.3 Ma
knickpoint at 1.1 Ma
>1.5 km uplift of the offshore forearc and western Coastal Cordillera
erosion arrive in the Principal Cordillera and fluvial excavation occurs in the Central Depression
horizontal scale
0
50
100 km

Figure 10

Table 5. Calculation of Crustal Shortening, Thickening and Uplift[a]

Model	Zone Affected by Shortening	Final Length of the Shortened Zone L	Shortening ΔL	Mean Final Crustal Thickness T of the Zone Affected by Shortening	Thickening ΔT	Uplift Δh[b]
1	Trench to Frontal Cordillera	330	32	40–50	2.7–3.4	0.63–0.79
2	eastern Coastal Cordillera, Principal Cordillera, and Frontal Cordillera	160	32	50–60	8.3–10.0	1.49–1.79

[a]Mean uplift affecting the zone comprised between the trench and the Frontal Cordillera (model 1 in section 6) and between the eastern Coastal Cordillera and the Frontal Cordillera (model 2).
[b]Calculated using equation (B3).

[52] As previously mentioned, the most likely model (model 2, Figure 10b) implies that regional uplift and deformation in the Principal Cordillera were coeval. However, the shortening accommodated between 10 and 4 Ma was only ~32 km at the latitude of Santiago [*Giambiagi and Ramos*, 2002]. Even though shortening could be underestimated, such a magnitude of shortening would produce 1.5–1.8 km of mean surface uplift from the eastern Coastal Cordillera to the Frontal Cordillera (see Table 5 and Appendix B). This uplift equals the minimum surface uplift estimated for the eastern Coastal Cordillera, but it is relatively similar to the mean uplift at 35°S. Unfortunately, there is no estimation for the magnitude of shortening at 35°S. In spite of this, we suspect that this should be lesser because crustal thickness is about 10 km minor than at 33°S [see *Tassara et al.*, 2006]. Therefore the crustal shortening occurring at this time could not explain completely the observed surface uplift.

[53] The establishment of the southern edge of the flat slab subduction zone (33°S) at ~10 Ma would have produced changes in the upper mantle material distribution beneath the mountain belt. This process probably induced material displacement to the south and to the southeast [cf. *Wagner et al.*, 2005], which could produce changes in the floatability of the continent [see *Yáñez et al.*, 2001, and references therein]. We agree with the fact that flat subduction should not significantly affect regions situated ~200 km to the south (i.e., at 35°S). However, this is consistent with the southward decrease in elevation of the mountain belt. Therefore it is reasonable to propose that surface uplift would have been mainly the result of tectonic shortening and partially as a consequence of the effects related to the flattening of the slab.

7. Summary and Conclusions

[54] On the basis of morphological analysis and fission track and radiometric data, we presented evidence for rapid and high magnitude regional uplift of the Andes of central Chile. Evidence can be synthesized as follows: (1) high-elevated peneplains in the eastern Coastal Cordillera and in the western Principal Cordillera and (2) more than 2 km of incision in the Principal Cordillera.

[55] Peneplains in the eastern Coastal Cordillera and in the western Principal Cordillera would have corresponded to the same surface prior to the onset of the uplift. Offset between them would be the result of the activity of the San Ramón-Pocuro fault, including its southward prolongation. This offset implies that this fault would have produced <1.1 km of relative upheaval on the Principal Cordillera at the latitude of Santiago and 800–600 m at 35°S. Most of the uplift of the eastern Coastal Cordillera and Principal Cordillera would have occurred during the same event.

[56] Peneplain elevations show that the eastern Coastal Cordillera underwent 2.1–1.5 km of surface uplift at the latitude of Santiago, and<1 km at 35°S. Peneplains and incision markers show that the western Principal Cordillera has been uplifted ~2 km, and the central Principal Cordillera and eastern Principal Cordillera were uplifted between 1.5 km (at 34°30′S) and >2.5 km (at 33°45′S).

[57] Incision rates show minimum values between 1.0–1.7 mm a^{-1} across the Principal Cordillera along a short period (~1–2 Ma). Incision occurred sooner in the western Principal Cordillera than in the eastern Principal Cordillera, which is evidence for the delay in the propagation of the erosion. Using incision markers, knickpoint retreat celerity ranges between 6 and 19 mm a^{-1}. Modeling using a stream power law for detachment-limited systems gives velocities of knickpoint retreat between 10 and 40 mm a^{-1} for the segment comprised from the paleocoast (western edge of the eastern Coastal Cordillera) to the western Principal Cordillera. This estimation shows that knickpoints arrived in the western Principal Cordillera 2–6 Ma after the onset of surface uplift, and >2 Ma later in the eastern Principal Cordillera. These results reveal that the erosional response to uplift could have been delayed 5–10 Ma. Therefore different methodologies based on erosional and sedimentary records that are commonly used to interpret ancient or recent uplift would need to be reevaluated.

[58] On the basis of our estimations, surface uplift would have begun between 10.5 and 4.6 Ma (central age at 7.6 Ma) and lasted about 2 Ma. Because our estimation for the onset of surface uplift is very rough, we proposed two models for the timing and the zones affected by surface uplift. The first proposition implies that surface uplift would have commenced shortly before 4 Ma affecting the zone comprised

from the offshore fore arc to the Principal Cordillera. The second model suggests that the western Coastal Cordillera and the offshore fore arc began to be uplifted after the uplift of the eastern Coastal Cordillera and Principal Cordillera. We consider that the second model is more reliable because three major tectonic events occurred at the same time in the study region, which could also explain the surface uplift. These processes are (1) the establishment of the southern edge of the flat subduction region at its present-day location at ~10 Ma, (2) the uplift of the Frontal Cordillera and out-of-sequence thrusting in the eastern central Principal Cordillera, and (3) high subsidence of the offshore fore arc and western Principal Cordillera. On the other hand, it has been previously proposed by other authors that the uplift of the offshore fore arc and western Principal Cordillera would have been a consequence of large sediment income in the trench. This process could be the end result of the erosion in response to the surface uplift.

[59] Concluding, the great surface uplift would be the result of the tectonic shortening that affected the eastern and central Principal Cordilleras between 8.5 and 4 Ma, and the influence produced by the flattening of the slab in the northern part of the study region.

Appendix A: Estimation of Mean Knickpoint Retreat Celerity

[60] Erosion in detachment-limited systems can be modeled by a stream power law, which relates the incision rate E with the drainage area A (as a proxy of the discharge) and the channel slope S [*Howard*, 1980]:

$$E = \frac{\partial z}{\partial t} = -KA^m S^n, \tag{A1}$$

where m and n are positive nondimensional constants and K is the dimensional coefficient of erosion. This relationship can be rewritten in the form of a nonlinear kinematic wave equation [e.g., *Rosenbloom and Anderson*, 1994; *Whipple and Tucker*, 1999]:

$$\frac{\partial z}{\partial t} = -KA^m S^{n-1}\left|\frac{\partial z}{\partial x}\right|, \frac{\partial z}{\partial x} < 0, \tag{A2}$$

where $C \approx KA^m S^{n-1}$ is the wave speed. From Hack's law, the drainage area can be approximated by the distance x downstream from the drainage divide along the main trunk:

$$A = k_a x^h, \tag{A3}$$

where k_a is a dimensional constant and h is the reciprocal of the Hack exponent. Combining (A2) with (A3), the wave speed equation can be reduced to one dimension:

$$C(x) = Kk_a^m x^{hm} S^{n-1}. \tag{A4}$$

[61] Considering $n = 1$, equation (A4) takes a simplified form

$$C(x) = Kk_a^m x^{hm}. \tag{A5}$$

[62] Given two points along the main river ($x = a$ and $x = b$ from the drainage divide, $a < b$), the average wave celerity is represented by

$$\overline{C}_{ab} = (b-a)/\left[\int_a^b C(x)^{-1}dx\right] = (b-a)\frac{KK_a^m(1-hm)}{(b^{1-hm}-a^{1-hm})} \tag{A6}$$

[63] Knowing the average wave speed between two points (b^* and a^*), the mean erodability constant K can be evaluated:

$$K = \frac{\overline{C}_{b^*a^*}}{(b^*-a^*)}\frac{b^{*1-hm}-a^{*1-hm}}{k_a^m(1-hm)}. \tag{A7}$$

[64] Inversely, knowing K it is possible to evaluate equation (A6) and thus extrapolate the result to other segments of the main rivers.

Appendix B: Calculation of Surface Uplift Due to Crustal Shortening

[65] Crustal thickening in mountain ranges mainly results from tectonic shortening. In a two-dimensional analysis, crustal thickening (ΔT) resulting from tectonic shortening (ΔL) can be calculated using the following relationship:

$$(L+\Delta L)\cdot(T-\Delta T) = L\cdot T \Leftrightarrow \Delta T = T\left(1-\frac{L}{L+\Delta L}\right), \tag{B1}$$

where L and T are the final crustal length and thickness, respectively. Surface uplift (Δh) resulting from Airy isostatic compensation after thickening (ΔT) is defined by

$$\Delta h = \frac{1}{5.6}\Delta T, \tag{B2}$$

considering normal crustal and mantle densities of 2.8×10^3 and 3.3×10^3 kg m^{-3}, respectively.

[66] Combining (B1) with (B2),

$$\Delta h = \frac{T}{5.6}\left(1-\frac{L}{L+\Delta L}\right) \tag{B3}$$

[67] **Acknowledgments.** This work was supported by the FONDECYT project 1030965, the Bicentennial Program in Science and Technology grant ANILLO ACT-18, and the INSU grant "Reliefs de la Terre. Impact du climat sur la dynamique du relief des Andes: quantification et modélisation." M. Farías's doctoral study at the Universidad de Chile and

Université Paul Sabatier has been supported by the Institut de Recherche pour le Développement (IRD). Some figures and analyses were made using GMT 4.1 [*Wessel and Smith*, 1998] and GRASS 6.2 (http://grass.itc.it). Morphological analysis was performed using SRTM 90 m DEM (http://seamless.usgs.gov) and GTOPO30 (http://edcdaac.usgs.gov/gtopo30/gtopo30.htm) digital topography. We thank our colleague Marcelo Araya, Compañía Minera Cenizas Alhué, and Sergio Cuevas for valuable help during fieldwork. Apatite to Zircon Inc. is acknowledged for rapid and thorough apatite and zircon fission track analyses. Useful discussion with Andrés Tassara, Gérard Hérail, Victor Maksaev, M. Pía Rodriguez, Marcia Muñoz, Alfonso Encinas, and Julien Babault helped develop and clarify our ideas. Constructive comments by Onno Oncken, Daniel Melnick, Alain Lavenu, and an anonymous reviewer led to significant improvements in the manuscript.

References

Abele, G. (1984), Derrumbes de montaña y morrenas en los Andes chilenos, *Rev. Geogr. Norte Grande*, *11*, 17–30.

Aguirre, L., G. Feraud, M. Vergara, J. Carrasco, and D. Morata (2000), $^{40}Ar/^{39}Ar$ ages of basic flows from the Valle Nevado stratifies sequence (Farellones Formation), Andes of central Chile, paper presented at IXth Congreso Geológico Chileno, Geol. Soc. of Chile, Puerto Varas, Chile, 31 July to 4 Aug.

Allmendinger, R. W. (1986), Tectonic development of the southeastern border of the Puna plateau, northwestern Argentina Andes, *Geol. Soc. Am. Bull.*, *97*, 1072–1082.

Araneda, M., M. S. Avendaño, and C. Merlo (2000), Modelo gravimétrico de la Cuenca de Santiago, etapa II final, paper presented at IXth Congreso Geológico Chileno, Geol. Soc. of Chile, Puerto Varas, Chile, 31 July to 4 Aug.

Arcos, R. (1987), Geología del Cuadrángulo Termas del Flaco, provincia de Colchagua, VI Región, Chile, thesis, 279 pp., Univ. de Chile, Santiago.

Babault, J., J. Van Den Driessche, S. Bonnet, S. Castelltort, and A. Crave (2005), Origin of the highly elevated Pyrenean peneplain, *Tectonics*, *24*, TC2010, doi:10.1029/2004TC001697.

Baeza, O. (1999), Análisis de litofacies, evolución depositacional y análisis estructural de la Formación Abanico en el área comprendida entre los ríos Yeso y Volcán, Región Metropolitana, thesis, 54 pp., Univ. de Chile, Santiago.

Beccar, I., M. Vergara, and F. Munizaga (1986), Edades K-Ar de la Formación Farellones en el Cordón del Cerro La Parva, Cordillera de los Andes de Santiago, *Chile, Rev. Geol. Chile*, *28–29*, 109–113.

Borde, J. (1966), *Les Andes de Santiago et Leur Avant-Pays: Etude de Géomorphologie*, 559 pp., Union Fr. d'Impression, Bordeaux, France.

Brüggen, H. (1950), *Fundamentos de la Geología de Chile*, 510 pp., Inst. Geogr. Mil., Santiago.

Burbank, D. W., J. Leland, E. Fielding, R. S. Anderson, N. Brozovic, M. R. Reid, and C. Duncan (1996), Bedrock incision, rock uplift and threshold hillslopes in the northwestern Himalayas, *Nature*, *379*, 505–510.

Charrier, R., and F. Munizaga (1979), Edades K-Ar de vulcanitas cenozoicas del sector cordillerano del río Cachapoal (34°15′ de latitud Sur), *Rev. Geol. Chile*, *7*, 41–51.

Charrier, R., A. R. Wyss, J. J. Flynn, C. C. Swisher, M. A. Norell, F. Zapatta, M. C. McKenna, and M. J. Novaceck (1996), New evidence for late Mesozoic-early Cenozoic evolution of the Chilean Andes in the upper Tinguiririca valley (35°S), central Chile, *J. South Am. Earth Sci.*, *9*, 1–30.

Charrier, R., O. Baeza, S. Elgueta, J. J. Flynn, P. Gans, S. M. Kay, N. Muñoz, A. R. Wyss, and E. Zurita (2002), Evidence for Cenozoic extensional basin development and tectonic inversion south of the flat-slab segment, southern central Andes,. Chile (33°–36°S. L.), *J. South Am. Earth Sci.*, *15*, 117–139.

Charrier, R., M. Bustamante, D. Comte, S. Elgueta, J. J. Flynn, N. Iturra, N. Muñoz, M. Pardo, R. Thiele, and A. R. Wyss (2005), The Abanico extensional basin: Regional extension, chronology of tectonic inversion, and relation to shallow seismic activity and Andean uplift, *Neues Jahrb. Geol. Palaeontol. Abh.*, *236*(1–2), 43–47.

Charrier, R., L. Pinto, and M. P. Rodríguez (2007), Tectono-stratigraphic evolution of the Andean orogen in Chile, in *Geology of Chile*, edited by T. Moreno and W. Gibbons, pp. 21–116, Geol. Soc., London.

Coira, B., J. Davidson, C. Mpodozois, and V. Ramos (1982), Tectonic and magmatic evolution of the Andes of northern Argentina and Chile, *Earth Sci. Rev.*, *18*, 303–332.

Cornejo, P., and G. Mahood (1997), Seeing past effects of re-equilibration to reconstruct magmatic gradient in plutons: La Gloria Pluton, central Chilean Andes, *Contrib. Mineral Petrol.*, *127*, 159–175.

Dalmayrac, B., and P. Molnar (1981), Parallel thrust and normal faulting in Peru and constraint on the state of stress, *Earth Planet. Sci. Lett.*, *55*, 473–481.

Daniels, J. M. (2002), Drainage network adjustment following channelization, Homochitto River Basin, Mississippi, in *Cultural and Physical Expositions: Geographic Studies in the Southern United States and Latin America*, *Geosci. Man Ser.*, vol. 36, edited by M. Steinberg and P. Hudson, pp. 291–308, La. State Univ. Press, Baton Rouge.

Deckart, K., A. H. Clark, C. Aguilar, R. Vargas, A. Bertens, J. K. Mortensen, and M. Fanning (2005), Magmatic and hydrothermal chronology of the giant Río Blanco porphyry copper deposit, central Chile: Implications of an integrated U-Pb and $^{40}Ar/^{39}Ar$ database, *Econ. Geol.*, *100*, 905–934.

Dorsey, R. J., and J. J. Roering (2006), Quaternary landscape evolution in the San Jacinto fault zone, peninsular ranges of southern California: Transient response to strike-slip fault initiation, *Geomorphology*, *73*(1–2), 16–32.

Elgueta, S., R. Charrier, R. Aguirre, G. Kieffer, and N. Vatin-Perignon (1999), Volcanogenic sedimentation model for the Miocene Farellones Formation, Andean cordillera, central Chile, paper presented at 4th International Symposium on Andean Geodynamics, Inst. de Rech. pour le Dév., Göttingen, Germany.

Encinas, A., J. P. Le Roux, L. Buatois, S. Nielsen, K. Finger, E. Fourtanier, and A. Lavenu (2006a), Nuevo esquema estratigráfico para los depósitos miopliocenos del area de Navidad (33°00′–34°30′S), Chile central, *Rev. Geol. Chile*, *33*, 221–246.

Encinas, A., V. Maksaev, L. Pinto, J. P. Le Roux, F. Munizaga, and M. Zentilli (2006b), Pliocene lahar deposits in the Coastal Cordillera of central Chile: Implications for uplift, avalanche deposits, and porphyry copper systems in the main Andean Cordillera, *J. South Am. Earth Sci.*, *20*, 369–381.

Encinas, A., K. L. Finger, S. N. Nielsen, A. Lavenu, L. A. Buatois, D. E. Peterson, and J. P. Le Roux (2007), Rapid and major coastal subsidence during the late Miocene in south-central Chile, *J. South Am. Sci.*, doi:10.1016/j.jsames.2007.07.001, in press.

Farías, M., D. Comte, and R. Charrier (2006a), Sismicidad superficial en Chile central: Implicancias para el estado cortical y crecimiento de los Andes Centrales Australes, paper presented at XIth Congreso Geológico Chileno, Univ. Católica del Norte, Antogafasta, Chile, 7–11 Aug.

Farías, M., R. Charrier, S. Carretier, J. Martinod, and D. Comte (2006b), Erosión versus tectónica en el origen de la Depresión Central de Chile central, paper presented at XIth Congreso Geológico Chileno, Univ. Católica del Norte, Antogafasta, Chile, 7–11 Aug.

Finger, K. L., S. N. Nielsen, T. Devries, A. Encinas, and D. E. Peterson (2007), Paleontologic evidence for sedimentary displacement in Neogene forearc basins of central Chile, *Palaios*, *22*, 3–16.

Fock, A., R. Charrier, M. Farías, V. Maksaev, M. Fanning, and P. P. Álvarez (2005), Deformation and uplift of the western Main Cordillera between 33° and 34°S, paper presented at 6th International Symposium on Andean Geodynamics, Inst. de Rech. pour le Dév., Barcelona, Spain.

Fuentes, F., M. Vergara, L. Aguirre, and G. Féraud (2002), Relaciones de contacto de unidades volcánicas terciarias de los Andes de Chile central (33°S): Una reinterpretación sobre la base de dataciones $^{40}Ar/^{39}Ar$, *Rev. Geol. Chile*, *29*, 207–225.

Gana, P., and R. Wall (1997), Evidencias geocronológicas $^{40}Ar/^{39}Ar$ y K-Ar de un hiatus Cretácico Superior-Eoceno en Chile central (33°–33°30′S), *Rev. Geol. Chile*, *24*, 145–163.

Gardner, T. W. (1983), Experimental study of knickpoint and longitudinal profile evolution in cohesive, homogeneous material, *Geol. Soc. Am. Bull.*, *94*, 664–672.

Giambiagi, L. B., and V. A. Ramos (2002), Structural evolution of the Andes between 33°30′ and 33°45′S, above the transition zone between the flat and normal subduction segment, Argentina and Chile, *J. South Am. Earth Sci.*, *15*, 99–114.

Giambiagi, L. B., V. A. Ramos, E. Godoy, P. P. Alvarez, and S. Orts (2003), Cenozoic deformation and tectonic style of the Andes, between 33° and 34° south latitude, *Tectonics*, *22*(4), 1041, doi:10.1029/2001TC001354.

Godoy, E., and L. Lara (1994), Segmentación estructural andina a los 33°–34°: Nuevos datos en la Cordillera Principal, paper presented at VIIth Congreso Geológico Chileno, Dep. de Cienc. de la Tierra, Univ. de Concepción, Concepción, Chile.

Godoy, E., G. Yáñez, and E. Vera (1999), Inversion of an Oligocene volcano-tectonic basin and uplift of its superimposed Miocene magmatic arc, Chilean central Andes: First seismic and gravity evidence, *Tectonophysics*, *306*, 217–326.

Gripp, A. E., and R. G. Gordon (2002), Young tracks of hotspots and current plate velocities, *Geophys. J. Int.*, *150*, 321–361.

Hack, J. T. (1957), Studies of longitudinal stream profiles in Virginia and Maryland, *U.S. Geol. Surv. Prof. Pap.*, *294*, 45–94.

Haq, B., J. Hardenbol, and P. Vail (1987), Chronology of fluctuating sea levels since the Triassic, *Science*, *235*, 1156–1167.

Haviv, I., Y. Enzel, K. Whipple, E. Zilberman, J. Stone, A. Matmon, and L. K. Fifield (2003), Knickpoint retreat and drawndown reach evolution along the arid escarpments of the Dead Sea Basin, *Geol. Soc. Am. Abstr. Programs*, *35*(6), 333.

Howard, A. D. (1980), Thresholds in river regimes, in *Thresholds in Geomorphology*, edited by D. R. Coates and J. D. Vitek, pp. 227–258, Allen and Unwin, Concord, Mass.

Isacks, B. L. (1988), Uplift of the central Andean plateau and bending of the Bolivian orocline, *J. Geophys. Res.*, *93*, 3211–3231.

Jordan, T. E., B. L. Isacks, R. W. Allmendinger, J. A. Brewer, V. Ramos, and C. J. Ando (1983), Andean

tectonics related to geometry of subducted Nazca plate, *Geol. Soc. Am. Bull.*, *94*, 341–361.

Kay, S. M., and C. Mpodozis (2001), Central Andes ore deposits linked to evolving shallow subduction systems and thickening crust, *GSA Today*, *11*, 4–9.

Kay, S. M., C. Mpodozis, V. Ramos, and F. Munizaga (1991), Magma source variations for mid-late Tertiary magmatic rocks associated with a shallowing subduction zone and thickening crust in the central Andes, *Spec. Pap. Geol. Soc. Am.*, *265*, 113–137.

Kay, S. M., E. Godoy, and A. Kurtz (2005), Episodic arc migration, crustal thickening, subduction erosion, and magmatism in the south-central Andes, *Geol. Soc. Am. Bull.*, *117*, 67–88.

Kurtz, A., S. M. Kay, R. Charrier, and E. Farrar (1997), Geochronology of Miocene plutons and exhumation history of the El Teniente region, central Chile (34°–35°S), *Rev. Geol. Chile*, *24*, 75–90.

Lamb, S., and P. Davis (2003), Cenozoic climate change as a possible cause for the rise of the Andes, *Nature*, *425*, 792–797.

Maksaev, V., M. Zentilli, F. Munizaga, and R. Charrier (2003), Denudación/alzamiento del Mioceno superior–Plioceno Inferior de la Cordillera de Chile Central (33°–35°S) inferida por dataciones por trazas de fisión en apatito de plutones miocenos, paper presented at Xth Congreso Geológico Chileno, Dep. de Cienc. de la Tierra, Univ. de Concepción, Concepción, Chile.

Maksaev, V., F. Munizaga, M. McWilliams, M. Fanning, R. Mathur, J. Ruiz, and M. Zentilli (2004), New chronology for El Teniente, Chilean Andes, from U/Pb, $^{40}Ar/^{39}Ar$, Re/Os and fission-track dating: Implications for the evolution of a supergiant porphyry Cu-Mo deposit, in *Andean Metallogeny: New Discoveries, Concepts, and Updates*, *Spec. Publ.*, vol. 11, edited by R. H. Sillitoe, J. Perelló, and C. E. Vidal, pp. 15–54, Soc. of Econ. Geol., Littleton, Colo.

Marshall, J. S., B. D. Idleman, T. W. Gardner, and D. M. Fisher (2003), Landscape evolution within a retreating volcanic arc, Costa Rica, Central America, *Geology*, *31*, 419–422.

Mather, A. E., M. Stokes, and J. S. Griffiths (2002), Quaternary landscape evolution: A framework for understanding contemporary erosion, southeast Spain, *Land Degrad. Rehabil.*, *13*, 89–109, doi:10.1002/ldr.484.

Mathur, R., J. Ruiz, and F. Munizaga (2000), Relationship between copper tonnage of Chilean base-metal porphyry deposits and Os isotope ratios, *Geology*, *28*, 555–558.

McInnes, B. I. A., et al. (2005), Thermal history analysis of selected Chilean, Indonesian and Iranian porphyry Cu-Mo-Au deposits, in *Super Porphyry Copper and Gold Deposits: A Global Perspective*, vol. 1, edited by T. M. Porter, pp. 27–42, PGC Publ., Adelaide, Australia.

Melnick, D., and H. P. Echtler (2006), Inversion of forearc basins in south-central Chile caused by rapid glacial age trench fill, *Geology*, *34*, 709–712.

Melnick, D., B. Bookhagen, H. P. Echtler, and M. R. Strecker (2006), Coastal deformation and great subduction earthquakes, Isla Santa Maria, Chile (37°S), *Geol. Soc. Am. Bull.*, *118*, 1463–1480.

Miller, K. G., M. A. Kominz, J. V. Browing, J. D. Wright, G. S. Mountain, M. E. Katz, P. J. Sugarman, B. S. Cramer, N. Christie-Blick, and S. F. Pekar (2005), The Phenerozoic record of global sea-level change, *Science*, *310*, 1293–1298.

Molnar, P. (2004), Late Cenozoic increase in accumulation rates of terrestrial sediment: How might climate change have affected erosion rates?, *Annu. Rev. Earth Planet. Sci.*, *32*, 67–89.

Nott, J., R. Young, and I. McDougall (1996), Wearing down, wearing back, and gorge extension in the long-term denudation of a highland mass: Quantitative evidence from the Shoalhaven Catchment, southeast Australia, *J. Geol.*, *104*, 224–232.

Nyström, J. A., M. A. Parada, and M. Vergara (1993), Sr-Nd isotope compositions of Cretaceous to Miocene volcanic rocks in central Chile: A trend toward a MORB signature and a reversal with time, paper presented at 2nd International Symposium on Andean Geodynamics, Inst. de Rech. pour le Dév., Oxford, U.K.

Oleskevich, D. A., R. D. Hyndman, and K. Wang (1999), The updip and downdip limits to great subduction earthquakes: Thermal and structural models of Cascadia, south Alaska, SW Japan, and Chile, *J. Geophys. Res.*, *104*, 14,965–14,992.

Pazzaglia, F. J., T. W. Gardner, and D. J. Merritts (1998), Bedrock fluvial incision and longitudinal profile development over geological time scales determined by fluvial terraces, in *Rivers Over Rocks: Fluvial Processes in Bedrock Channels*, *Geophys. Monogr. Ser.*, vol. 107, edited by K. J. Tinkler and E. E. Wohl, pp. 207–235, AGU, Washington, D. C.

Phillips, J. D. (2002), Erosion, isostatic response, and the missing peneplains, *Geomorphology*, *45*(3–4), 225–241.

Phillips, W. M., D. C. Commins, S. Gupta, and P. W. Kubik (2004), Rates of knickpoint migration and bedrock erosion from cosmogenic ^{10}Be in a landscape of active normal faulting, *Geophys. Res. Abstr.*, *6*, 06582.

Rabbia, O. M., M. Reich, L. B. Hernández, R. King, and L. López-Escobar (2003), High Al-TTG-like suite at the El Teniente Porphyry Copper Deposit, Chile, paper presented at IXth Congreso Geológico Chileno, Soc. Geol. de Chile, Puerto Varas, Chile.

Ramos, V. A., E. O. Cristallini, and D. J. Pérez (2002), The Pampean flat-slab of the Central Andes, *J. South Am. Earth Sci.*, *15*(1), 59–78, doi:10.1016/S0895-9811(02)00006-8.

Rauld, R., G. Vargas, R. Armijo, A. Ormeño, C. Valderas, and J. Campos (2006), Cuantificación de escarpes de falla y deformación reciente en el frente cordillerano de Santiago, paper presented at XIth Congreso Geológico Chileno, Univ. Católica del Norte, Antogafasta, Chile, 7–11 Aug.

Reich, M., M. A. Parada, C. Palacios, A. Dietrich, F. Schulz, and B. Lehmann (2003), Adakite-like signature of late Miocene intrusions at the Los Pelambres giant porphyry copper deposit in the Andes of central Chile: Metallogenic implications, *Miner. Deposita*, *38*, 876–885.

Righter, K. (1997), High bedrock incision rates in the Atenguillo river valley, Jalisco, western Mexico, *Earth Surf. Processes Landforms*, *22*, 337–343.

Rodríguez, M. P., L. Pinto, M. Farías, and G. Hérail (2007), Recent uplift of the coastal border of central Chile and its relationship with subduction factory, paper presented at 2nd International Geological Congress on the Southern Hemisphere, Dep. de Geol., Univ. de Chile, Santiago, Chile, 19–20 Nov.

Rosenbloom, N. A., and R. S. Anderson (1994), Hillslope and channel evolution in a marine terraced landscape, Santa Cruz, California, *J. Geophys. Res.*, *99*, 14,013–14,030.

Schlunegger, F., G. Zeilinger, A. Kounov, F. Kober, and B. Husser (2006), Scale of relief growth in the forearc of the Andes of northern Chile (Arica latitude, 18°S), *Terra Nova*, *18*(3), 217–223.

Seidl, M. A., and W. E. Dietrich (1992), The problem of channel erosion into bedrock, *Catena Suppl.*, *23*, 101–124.

Seidl, M. A., W. E. Dietrich, and J. W. Kirchner (1994), Longitudinal profile development into bedrock: An analysis of Hawaiian channels, *J. Geol.*, *102*, 457–474.

Servicio Geológico Minero Argentino (1997), Mapa geológico de la República Argentina, scale 1:2,500,000, Buenos Aires.

Servicio Nacional de Geología y Mineŕa (2002), Mapa geológico de Chile, *Map M61*, scale 1:1,000,000, Santiago.

Simon, A., and R. E. Thomas (2002), Process and forms of an unstable alluvial system with resistant, cohesive streambeds, *Earth Surf. Processes Landforms*, *27*, 699–718.

Skewes, M. A., and C. Holmgren (1993), Solevantamiento andino, erosion y emplazamiento de brechas mineralizadas en el depósito de cobre porfídico Los Bronces, Chile Central (33(S): Aplicación de termometría de inclusiones fluidas, *Rev. Geol. Chile*, *20*, 71–84.

Skewes, M. A., and C. R. Stern (1996), Late Miocene mineralized breccias in the Andes of central Chile: Sr and Nd isotopic evidence for multiple magmatic sources, in *Andean Copper Deposits: New Discoveries, Mineralization, Styles, and Metallogeny, Spec. Publ.*, vol. 5, pp., 33–41, Soc. of Econ. Geol., Littleton, Colo.

Somoza, R. (1998), Updated Nazca (Farallon)–South America relative motions during the last 40 Myr: Implications for mountain building in the central Andean region, *J. South Am. Earth Sci.*, *11*, 211–215.

Stern, C. R., and M. A. Skewes (1995), Miocene to present magmatic evolution at the northern end of the Andean Southern Volcanic Zone, central Chile, *Rev. Geol. Chile*, *22*, 261–272.

Stern, C. R., and M. A. Skewes (2004), Origin of giant Miocene and Pliocene Cu-Mo deposits in central Chile: Role of ridge subduction, decreased subduction angle, and long-lived, batholith size, open-system magma chambers, in *Super Porphyry Copper and Gold Deposits: A Global Perspective*, vol. 1, edited by T. M. Porter, pp. 65–83, PGC Publ., Adelaide, Australia.

Stern, C. R., H. Amini, R. Charrier, E. Godoy, F. Hervé, and J. Varela (1984), Petrochemistry and age of rhyolitic pyroclastic flows which occur along the drainage valleys of the Río Maipo and Río Cachapoal (Chile) and the Río Yaucha and Río Papagayos (Argentina), *Rev. Geol. Chile*, *23*, 39–52.

Tassara, A., H.-J. Götze, S. Schmidt, and R. Hackney (2006), Three-dimensional density model of the Nazca plate and the Andean continental margin, *J. Geophys. Res.*, *111*, B09404, doi:10.1029/2005JB003976.

Thomas, H. (1958), *Geología de la Cordillera de la Costa entre el valle de la Ligua y la cuesta Barriga*, 86 pp., Inst. de Invest. Geol., Santiago.

Tucker, G. E., and K. X. Whipple (2002), Topographic outcomes predicted by stream erosion models: Sensitivity analysis and intermodel comparison, *J. Geophys. Res.*, *107*(B9), 2179, doi:10.1029/2001JB000162.

Vergara, M., and R. Drake (1978), Edades potasio-argón y su implicancia en la geología regional de Chile, *Comunicaciones*, *23*, 1–11.

Vergara, M., R. Charrier, F. Munizaga, S. Rivano, P. Sepúlveda, R. Thiele, and R. Drake (1988), Miocene volcanism in the central Chilean Andes (31°30′S–34°35′S), *J. South Am. Earth Sci.*, *1*, 199–209.

Vergara, M., D. Morata, R. Villaroel, J. Nyström, and L. Aguirre (1999), $^{40}Ar/^{39}Ar$ ages, very low-grade metamorphism and geochemistry of the volcanic rock from "Cerro El Abanico", Santiago Andean cordillera (33°30′S, 70°30′–70°25′W), paper presented at 4th International Symposium on Andean Geodynamics, Inst. de Rech. pour le Dév., Göttingem, Germany.

Wagner, L. S., S. Beck, and G. Zandt (2005), Upper mantle structure in the south central Chilean subduction zone (30° to 36°S), *J. Geophys. Res.*, *110*, B01308, doi:10.1029/2004JB003238.

Wall, R., P. Gana, and A. Gutiérrez (1996), Mapa geológico del area de San Antonio, *Map 2*, 19 pp., Serv. Nac. Geol. y Min, Santiago.

Wessel, P., and W. H. F. Smith (1998), New version of the generic mapping tools released, *Eos Trans. AGU*, *79*, 579.

Whipple, K. X., and G. E. Tucker (1999), Dynamics of the stream-power river incision model: Implications for height limits of mountain ranges, landscape response timescales, and research needs, *J. Geophys. Res.*, *104*, 17,661–17,674.

Yáñez, G., and J. Cembrano (2004), Role of viscous plate coupling in the late Tertiary Andean tectonics, *J. Geophys. Res.*, *109*, B02407, doi:10.1029/2003JB002494.

Yáñez, G., C. R. Ranero, R. Von Huene, and J. Díaz (2001), Magnetic anomaly interpretation across the southern central Andes (32°–34°S): The role of the Juan Fernández Ridge in the late Tertiary evolution of the margin, *J. Geophys. Res.*, *106*, 6325–6345.

J. Cáceres, D. Campbell, R. Charrier, M. Farías, and A. Fock, Departamento de Geología, Universidad de Chile, Plaza Ercilla 803, Box 13518, E-21 Santiago, Chile. (mfarias@dgf.uchile.cl)

S. Carretier and J. Martinod, Laboratoire de Mécanismes et Transferts en Géologie, IRD, CNRS, Université de Toulouse, 19 av E Berlin, F-31400 Toulouse, France.

D. Comte, Departamento de Geofísica, Universidad de Chile, Avenida Blanco Encalada 2002, 651-1227 Santiago, Chile.